Variations in radiosensitivity of breast cancer and normal breast cell lines using a 200MeV clinical proton beam.

by

Peter Clark du Plessis
193062119

Dissertation submitted in fulfilment of the requirements for the degree

Master of Science in Radiography: Radiation Therapy
in the Faculty of Health and Wellness Sciences
at the Cape Peninsula University of Technology

Supervisor: Ms Neo Seane
Co-supervisor: Dr Charlot Vandevoorde and Ms Xanthene Muller

Bellville Campus
Date submitted (October 2018)

DECLARATION

I, Peter Clark du Plessis, declare that the contents of this thesis titled **Variations in radiosensitivity of breast cancer and normal breast cell lines using a 200MeV clinical proton beam** represent my own unaided work, and that the thesis has not previously been submitted for academic examination towards any qualification. Furthermore, it represents my own opinions and not necessarily those of the Cape Peninsula University of Technology.

31 October 2018

Signed Date

ABSTRACT

Background: Breast cancer is one of the most commonly diagnosed among woman in South Africa, and a more resilient effort should be focused on treatment improvements. Worldwide, proton therapy is increasingly used as a radiation treatment alternative to photon therapy for breast cancer, mostly to decrease the risk for radiation-induced cardiovascular toxicity. This *in vitro* study aims to determine a better understanding of the radiosensitivity of both tumour and normal breast cell lines to clinical proton irradiation. In addition, we propose to investigate whether the increase in linear energy transfer (LET) towards the distal part of the proton beam results in an increase in relative biological effectiveness (RBE) for both cell lines.

Methods: Malignant (MCF-7) and non-malignant (MCF-10A) breast cells were irradiated at different water equivalent depths in a 200 MeV proton beam at NRF iThemba LABS using a custom-made Perspex phantom: the entrance plateau, 3 points on the Bragg peak, the D80% and the D40%. A cytokinesis-block Micronucleus (CBMN) assay was performed and Micronuclei (MNi) were manually counted in binucleated cells (BNCs) using fluorescent microscopy. Reference dosimetry was carried out with a Markus chamber and irradiations were performed with a clinical proton beam generated at NRF iThemba LABS that was degraded to a R50 (half-value depths) range of 120 mm, with a field size of 10 cm x 10 cm and a 50 mm SOBP. The phantom could be adjusted to accommodate different perspex plates depending on the depth required within the proton beam. Cells were then exposed to 0.5, 1.0, 2.0, 3.0 and 4.0 Gy doses for each cell line independently and for each dose point.

Results and Discussion: For the CBMN results, a program was developed on Matlab platform to calculate the 95% confidence ellipse on the co-variance parameters α and β. These values were determined by fitting the linear quadratic dose response curve to the average number of radiation induced MNi per 1000 BN cells. The ellipse region around a coordinate (the average MN frequency) for both MCF-7 and MCF-10A cells at the plateau region was defined by the mean estimate of the α-value and the β-value that were plotted on the X-axis and Y-axis respectively. The ratio of the two parameters, α/β, is a measure of the impact of fractionation to determine the biological effective dose. In fractionated proton therapy, the MCF10A cells will repair less between two fractions compared to the MCF7 cells. This is not an indication of therapeutic gain from a fractioned treatment protocol. For this reason, the hypofractionated stereotactic treatment protocols that can be applied with protons could be to the befit of the breast cancer patient. The above argument is based only on the radiosensitivity of the two cell lines exposed in the plateau region. Further analysis of the 95% confidence ellipse of both cell lines also showed a clear increase of the alpha value toward the distal portion of the beam and indicates an increase in energy transfer in this region. The gradual increase in α and β parameters with depth for protons for both cells is of clinical importance, since it implicates a non-homogeneous dose within the targeted area and an unwanted high dose behind the targeted area. Distal energy modulation could be investigated especially with larger breast tumours. RBE was calculated as the ratio of the dose at the different positions to the dose at the entrance plateau position (reference) to obtain an equal level of biological effect. A statistically significant difference in radiosensitivity could be observed between malignant and non-malignant cells at all positions ($p<0.05$). The variation in RBE was between 0.99 to 1.99 and 0.92 to 1.6 for the MCF-7 and MCF10A cell respectively.

Conclusions: There is a variation in RBE along the depth-dose profile of a clinical proton beam. In addition, there is difference in radiosensitivity between the cancerous cells and the normal breast cells. While this study highlights a variation in sensitivity between cells it could be used by the modelling community to further develop biologically motivated treatment planning for proton therapy.

Keywords: Breast cancer, proton therapy, Cytokinesis-block micronucleus assay; MCF-7 cells, MCF-10A cells, radiobiology, RBE, hypofractionation

ACKNOWLEDGEMENTS

I would first like to thank my thesis advisor Dr Charlot Vandevoorde, a true expert in this field and indeed a ‘cool’ supervisor (with her perfectionistic approach) that truly inspires me.

The door to Prof Kobus Slabbert’ office was always open whenever I ran into a trouble spot or had a question about my research.

Dr Shankari Nair that consistently allowed this paper to be my own work, but steered me in the right the direction whenever she thought I needed it.

I would also like to thank Xanthene Muller – your Lab skills are Marvel-connected and Neo Seane – my smooth logistics-expert and mentor.

A special thank you to all those that helped behind the scenes, whether in a passage or the tearoom to share you knowledgeable input.

Thank you Christo van Tubbergh and Phillip Beukes with your ‘mad tricks’ in MathLAB.

Last, but definitely not least, my wife Shantal and daughter Allison – you guys are my world, words can’t describe how much I appreciate you both.

The financial assistance of the National Research Foundation towards this research is acknowledged. Opinions expressed in this thesis and the conclusions arrived at, are those of the author, and are not necessarily to be attributed to the National Research Foundation.

DEDICATION

I dedicate this work to my wife and daughter – with their encouragement, warmth and love is what made me able to achieve attainment.

TABLE OF CONTENTS

LIST OF FIGURES

LIST OF TABLES

LIST OF EQUATIONS

List of Symbols and Abbreviations

3-DCRT	3-dimensional conformal radiation therapy
7-AAD	7-amino-actinomycin D
α	Alpha
β	Beta
ɣ	Gamma
ɣH2AX	Phosphorylated H2AX
%	Percentage
Gy	Gray
µL	Microlitre
mL	Millilitre

A

ANOVA	Analysis of variance
AO	Acridine Orange

B

BN (C)	Binucleated (Cells)
BrdU	Bromodeoyuridine
BSRT	Breast stereotactic radiotherapy

C

CBMN	Cytokinesis-block micronucleus assay
cGy	CentiGray
CHO-K1	Chinese Hamster Ovary cells
Cyt-B	Cytochalasin-B

D

DMEM	Dulbecco's Modified Eagle Medium
DNA	Deoxyribonucleic acid
DSB(s)	Double strand break(s)
DAPI	4', 6-diamidino-2-phenylindole

E

e.g.	Example
EGF	Epidermal Growth Factor
eV	Electron Volt

F

FBS	Fetal bovine serum
Fig	Figure
FITC	Fluorescein isothiocyanate

G

G (0,1 and 2)	Gap phase (0,1 and 2)

H

H2AX	H2A histone family, member X
HT	Helical tomotherapy

I

IR	Ionising radiation
IAEA	International Atomic Energy Agency
ICRU	International Commission on Radiation Units and Measurements
IMRT	Intensity-modulated radiotherapy

J

J	Joule

K

KCl	Potassium Chloride
keV	Kiloelectron volts
keV/µm	Kiloelectron volts/micrometre
K-MT(s)	Kinecochores microtubule(s)
kV	Kilovoltage

L

LET	Linear energy transfer

M

M phase	Mitosis phase
MCF-7	Human breast adenocarcinoma cell line
MCF-10A	Non-tumourgenic human breast epithelial cell line
MN(i)	Micronucleus (micronuclei)
MNF	Micronucleus Frequency (Micronuclei Frequencies)
MeV	Mega electron-volts
MLC	Multileave collimators

MV	Megavolts
MWIC	Multi-wire ionisation chamber

N

NTCP	Normal tissue complication probability

P

PBS	Pencil beam scanning proton therapy
PPT	Passive scattering proton therapy
PT	Proton Therapy
PTCOG	Particle Therapy Co-operative Group

R

R50	Half-value depth
RBE	Relative biological effectiveness
rpm	Revolutions per minute
RT	Radiotherapy

S

S -phase	Synthesis phase
SOBP	Spread Out Bragg Peak
SSB(s)	Single-strand break(s)

T

TCP	Tumour control probability

V

VMAT	Volumetric modulated arc therapy

W

WHO	World Health Organisation

CHAPTER 1: BACKGROUND AND RATIONALE

***Overview**: Background information about proton radiation therapy and radiobiology are discussed during this opening section. This will include primary objectives, hypothesis and a brief overview to the general approach, specific aims, methodology and significance of this research.*

1.1 Introduction

Breast cancer is at a steady increase among women with an age-adjusted incidence rate of 31.4 per 100 000 women and a lifetime risk of 1 in 29 (Murugan, Dickens, Pisa, McCormack, Joffe, Jacobson, ans Cubasch; 2014). The global estimate stressed that almost 40% of woman diagnosed in 2012 died of the disease (Rayne and Benn, 2017). Survival rates are currently at 89% for breast patients who present with metastatic disease before 5 years after treatment in the United States of America (Chang *et al.*, 2018). However, in South Africa the mean metastasis-free survival rate in 2016 was at only 65% (Parag and Buccimazza, 2016). Based on the breast cancer policy in South Africa, breast cancer patients must be monitored regularly and at least once a year after the second year of treatment (Narod, Iqbal and Miller, 2015), but unfortunately due to most patients residing in rural areas this still remains a challenge and only 6.3% of patients are followed up with yearly mammograms, while 40.6% of mammography follow-ups gets delayed (Parag and Buccimazza, 2016). Research for a more effective initial approach to treat breast cancer patients in South Africa therefore needs to be highlighted. Radiation therapy, unfortunately also allows for radiation to unwanted structures and may be a key risk factor for developing subsequent contralateral breast cancer (Jaskowiak, 2014).

Although radiation therapy plays an essential role in cancer treatment it is based on the balance between cure and toxicity (Barnett *et al.*, 2009). The prescribed dose of radiation is aimed at destroying tumour cells while keeping the dose to the normal surrounding tissues within tolerance limits in order to reduce radiation therapy induced side effects (Emami, 2013). Different ionising radiation types can be used in radiation therapy based on their individual dose characteristics to achieve a preferred outcome. X-ray (or photon) based radiation therapy is still the conventional modality used in radiation oncology practice around the world. Although particle therapy was developed at scientific accelerator laboratories and remained a niche within radiation oncology during the last few decades, the clinical application of proton therapy (PT) has been rapidly increasing over the last few years (Hill-Kayser, Both and Tochner, 2011). According to the latest data of the Particle Therapy Co-operative Group (PTCOG), 81 PT facilities are in clinical operation at the moment, 48 centres are under construction and another 24 facilities are in planning stage (PTCOG, 2018). Between 1954 and 2016, more than 149 000 patients have been treated with PT globally (Jermann, 2017).

1.1.1 Proton Therapy for Breast Cancer

The clinical rationale for PT is primarily motivated by the inverted depth-dose profile of protons compared to photons (Figure 1.1). The depth-dose curve of photons is characterised by a decrease in energy deposition with increasing depth after a short build-up. Protons deposit a low dose in the entrance channel (plateau) followed by a steep increase and sharp dose fall-off towards the end of their range in the so-called ‘Bragg peak’. Beyond which point, no radiation dose is deposited. A series of weighted pristine peaks result in a spread-out Bragg peak (SOBP) which covers the treatment volume.

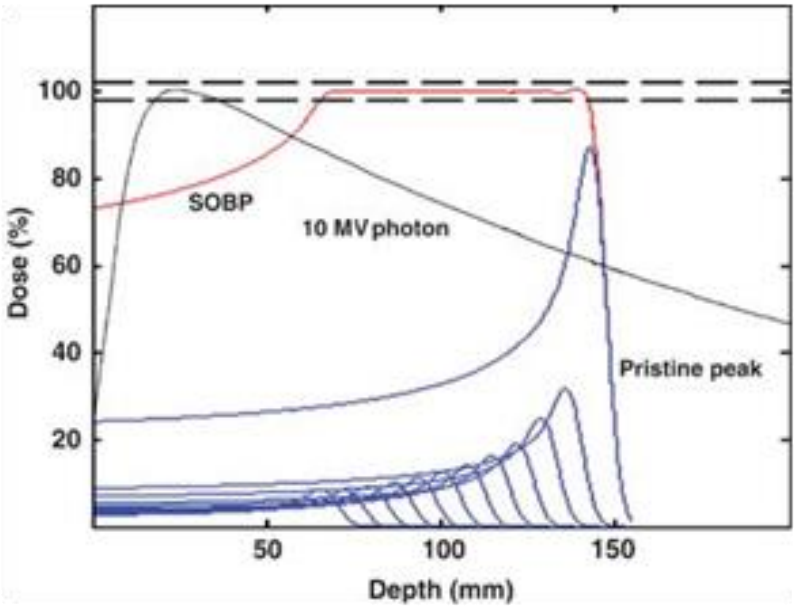

Figure 1.1: Depth dose distribution of proton and photon beams.
Depth–dose distributions for a proton spread-out Bragg peak (SOBP, red), pristine Bragg peaks (blue), and a 10 MV photon beam (black) (Levin *et al.*, 2005)

This unique property of protons can be effectively used by matching the range where protons mainly deposit their energy within the location of the tumour. In other words, the success of PT is due to the possibility to deliver the desired radiation dose in a broad, flat peak, where the flat section corresponds to the extent of the tumor (Figure 1.2), while reducing the radiation dose and damage to surrounding healthy organs and tissues.

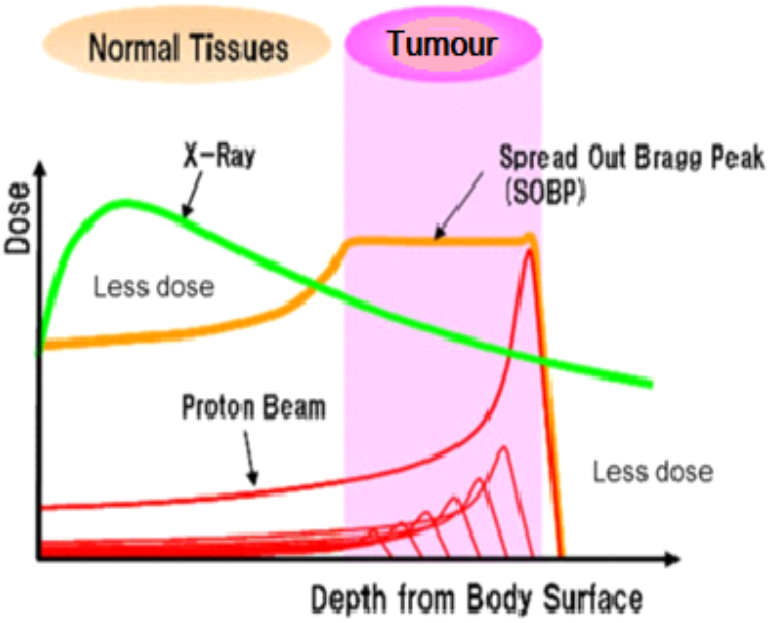

Figure 1.2: X-ray and proton dose distributions as a function of depth.
X-ray and proton energy deposition as a function of the body surface and depth illustrating how the maximum proton dose is spread out over the tumour. (Wroe, Bush and Slater, 2014).

The significant decrease of the dose to non-target tissues compared to conformal radiotherapy (RT) procedures such as intensity modulated radiation therapy (IMRT), is particularly important for the

treatment of tumours close to critical structures. (Dennis *et al.*, 2013). These critical structures vary based on which site within the body is being treated and side effects can range from insignificant to extremely severe. When comparing breast cancer treatment plans for PT with conventional RT it is evident that the energy distribution of protons into tissue can be more precisely directed and controlled. Therefore, PT creates the ability to reduce long-term side effects, especially in breast cancer patients due to its ability to minimise exposure to the heart and lungs (Figure. 1.3) (MacDonald, Jimenez, *et al.*, 2013). From tumour control probability (TCP) and normal tissue complication probability (NTCP) calculations, it was noted that PT is advantageous over conventional radiation therapy including photon IMRT (Miralbell, Lomax and Russo, 1997; Fuss et al., 2000).

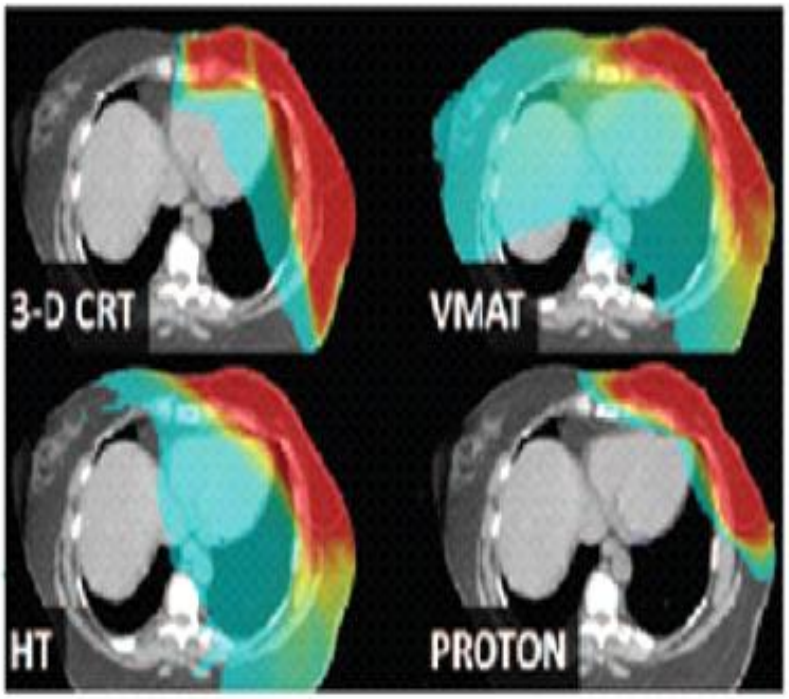

Figure 1.3: Treatment planning comparison displaying different dose distributions for different treatment modalities.
A treatment planning comparison using a colour-wash display (above 50% dose in red, 50% dose in yellow and below 50% dose in blue) for a breast carcinoma patient based on 3-dimensional conformal radiation therapy (3-DCRT), volumetric modulated arc therapy (VMAT), helical tomotherapy (HT) and proton therapy dose distribution. Note the absence of a significant exit dose for protons (Fagundes et al., 2015).

The pronounced dosimetric advantages of protons, the increased clinical experience and technological advances have resulted in PT slowly becoming an established alternative to conventional RT for the treatment of specific types of cancers like breast cancer and paediatric tumours (Hug and Slater, 1999; Cuaron, MacDonald and Cahlon, 2016). One of the major concerns for breast cancer radiation therapy with photons, is the potential increase in cardiac mortality related to radiation exposure to the heart (Early Breast Cancer Trialists Collaborative Group (EBCTCG)*, 2005; Hooning *et al.*, 2006; Darby *et al.*, 2013). Results from clinical trials based on cardiac mortality have indicated that the use of PT especially for early breast cancer patients either before or after mastectomy is beneficial to reduce cardiac morbidity (Lomax *et al.*, 2004; MacDonald, Patel, *et al.*, 2013; Strom and Ovalle, 2014). As mentioned before, this is primarily due to the superior physical characteristics of protons compared to photons, resulting in a reduction of the radiation dose to the heart (Taghian et al. 2006; Kozak et al. 2006 & Wang et al. 2011). This may reduce the cardiac mortality in left breast cancer survivors receiving radical radiation therapy, thus positively impacting breast cancer survival rates (Ares *et al.*, 2010; MacDonald, Patel, *et al.*, 2013; Xu *et al.*, 2014).

Despite the growing use of PT and a good understanding of the physical aspects, the radiobiological aspects have been underexplored and underexploited. Although many principles of radiation biology are shared between protons and photons, the vast majority need further investigation. A better understanding of the unique radiobiological characteristics of protons would augment current treatment strategies, both to enhance therapeutic effectiveness and to quantify risks related to PT (Girdhani, Sachs and Hlatky, 2013). A recent review of Corbin and Mutter gives a comprehensive overview of the potential challenges and areas of ongoing research that will ultimately establish the role of PT for breast cancer in the years ahead (Corbin and Mutter, 2018):

- *Target localisation*: The intentional or incidental irradiation of the axilla as a component of whole breast irradiation in conventional photon-based radiotherapy, might contribute to the low rate of axillary failure. Due to the rapid dose fall off in PT, there will be a decrease in the axillary dose which should be taken into account in planning if targeting is needed.
- Protons are much more sensitive to *treatment uncertainties*, such as changes in target volume over the course of treatment. Measures should be taken during treatment planning, setup and treatment
- *Relative biological effectiveness* (RBE): Emerging data suggest that the RBE of protons is greater at the distal end of the proton range, which means that the use of a generic proton RBE of 1.1 in clinical practice is not justified (see Section 1.2)
- PT has a *higher treatment expenses* due to the high capital investment and cost-effectiveness studies are ongoing for specific indications.

1.1.2 Relative Biological Effectiveness of Protons

The degree of damage caused by ionising radiation depends on the absorbed dose and on the radiation quality. Variances in the biological effects of different radiation types can be described in terms of the relative biological effectiveness (RBE). When treating patients with protons, the difference in the biologic effect for a given dose relative to photons must be considered for prescription doses as well as dose constraints. This is done through the use of the RBE (Paganetti *et al.*, 2002). The RBE is defined as the ratio of the doses required by two radiations to cause the same level of biologic effect as seen in Equation 1 (Sorensen, Overgaard and Bassler, 2011; Carante and Ballarini, 2016).

The general equation for RBE is:

Equation 1-1: Equation to calculate the relative biological effectiveness for the same effect for different radiation modalities.

$$\mathrm{RBE} = \frac{Dose_{reference\ radiation}}{Dose_{test\ radiation}}$$

RBE depends on numerous influences:

- Linear Energy Transfer (LET) defined as the average rate at which charged particles deposit their energy in the absorbing medium per unit distance (Paganetti *et al.*, 2002) (see Section 1.4),
- Beam energy (Abolfath *et al.*, 2017),
- Particle nuclear charge (Jones, 2015),
- Multiple biological factors that influence DNA repair capacity and radiosensitivity in different cellular types and tissues (Lühr *et al.*, 2018)

Historically, a generic value of 1.1 as the standard proton dosimetry protocol (used in radiation treatment planning) and was introduced to estimate the photon dose that would produce the same therapeutic effect as the proton absorbed dose given under identical conditions (Newhauser, 2009).

Conventionally, dose in PT is prescribed by scaling up the physical dose by 10% to accommodate for the RBE of 1.1 and ignoring any variation due to the increase in LET towards the end of the proton range.

Disregarding RBE variations could lead to sub-optimal proton plans, resulting in lower doses to the tumour and 'hot spots' in organs at risk (Wedenberg and Toma-Dasu, 2014). The extension of the bio-effective range due to variations in RBE, was illustrated in a study, in which 10 patients treated with PT for lumbar tumours, demonstrated an average overshoot of up to 1.9 mm in the lumbar spine from MRI data (Gensheimer *et al.*, 2010). This overshoot of the proton beam in the lumbar region ranged between (0.8–3.1 mm) and can also increase up to 4mm based on the extension of the SOBP bearing in mind that SOBP extension is much larger for breast patients (Corbin and Mutter, 2018) Range uncertainty also to increase up to 5% depending on the tissue type (Yang *et al.*, 2012). These studies point to the importance of the increase in RBE in the distal edge and if not accounted for in breast cancer PT, this range extension could result in greater toxicity to the ribs, lung and heart (Corbin and Mutter, 2018). Large variations are observed in published data sets on RBE values for different cell types, with most data referring to cell survival (Paganetti, 2014). It is well known that RBE values change significantly for different cells/tissues leading to a variation in cell sensitivity to radiation (Lühr *et al.*, 2018) and this is expected to be higher for non-lethal endpoints (Ando and Kase, 2009). In conclusion, the variation in RBE could have an unwanted effect on both tumour and normal surrounding healthy tissue (Jones, 2016). The debate on variable versus constant RBE of 1.1 in PT treatment planning is still ongoing (Sorensen, Overgaard and Bassler, 2011).

1.1.3 Linear Energy Transfer (LET)

Ionising radiation deposits energy in the form of ionisations along the track of the ionising particle. The spatial distribution of these ionisation events is associated to the radiation type (Tommasino and Durante, 2015). The term linear energy transfer (LET) defines the average rate at which charged particles deposit energy in the absorbing medium per unit distance (keV/µm) (Paganetti *et al.*, 2002). X-rays and gamma-rays are examples of low-LET radiation since it produces sparse ionisations separated by relative long distances while neutrons and alpha-particles are examples of high-LET radiation that produces ionisations over a very short distance (Figure 1.4) (Whalen *et al.*, 2008). Large amounts of ionizations in a short distance produces a higher, more complex biological damage which is more difficult to repair compared to less ionisations over a longer distance (Mason *et al.*, 2011). Therefore, the RBE will increase as the ionisation density or LET of the radiation type increases (Tommasino and Durante, 2015). Variation in LET is therefore directly linked to a variation in the radiobiological response of the cell (Barendsen, 1994; Grassberger et al., 2011). Belli et al. showed a clear increase in RBE when human normal and tumour cell lines were exposed to protons with increasing LET (Belli et al., 2000).

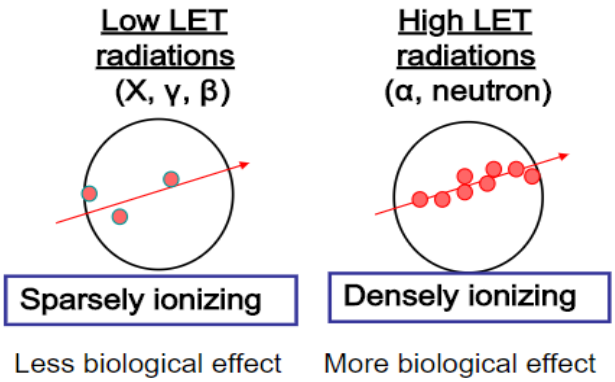

Figure 1.4: Ionisations for low and high LET radiations.
The more densely the ionizations are the higher biological damage (Chuai *et al.*, 2012).

1.1.4 Radiosensitivity

Radiosensitivity is the response of the type of tissue to irradiation and varies between normal tissues and tumours. Identifying this variation when treating breast cancer with proton irradiation could be of tremendous clinical benefit. The ability to repair radiation damage, hypoxia conditions, growth fraction and cell cycle position are all factors that could influence radiosensitivity. Unfortunately, no radiobiological assay has been exclusively identified that could be suitable to evaluate radiosensitivity for routine clinical use. Both *in vitro* and *in vivo* studies has added to a better understanding of cell and tissue responses to radiation (Joksic *et al.*, 2000; Smit, 2005; Fenech, 2007; Vral, Fenech and Thierens, 2011).

In vitro models can be used to predict and study in vivo tissue radiosensitivity and it reflects the relative susceptibility of cells, tissues and organs to the harmful effects of ionizing radiation (Hall and Cox, 2010). The radiosensitivity of cells can be investigated by either measuring the fraction of cells surviving a particular radiation dose (Begg, 2010), or measuring the fragments broken off from the chromosome after radiation (Scott *et al.*, 1999; Rothfuss *et al.*, 2000). Other methods include molecular approaches and can consist of DNA repair studies (McMahon *et al.*, 2016) or different cytogenetic procedures (Terzoudi and Pantelias, 2006). Radiosensitivity also varies throughout the cell cycle, such that the; late S-phase is most radioresistant, while G2/M phase is most radiosensitive and the G1 phase is intermediate (Hall, 1985; Gravina *et al.*, 2010). Furthermore, cells that divide frequently are more radiation-sensitive than those that divide rarely for most cells (Yashar, 2012). Quantifying sensitivity to irradiation can allow radiation dose escalation without increased normal tissue complications when treating breast cancer.

1.2 Research Aim

This study aimed to give a better understanding of the effect of proton radiation to breast cancer cells and clarify whether a radiation sensitivity variation exists and hence a variation in RBE for both tumour and normal breast cell lines in response to the 200 MeV proton beam. This study is in line with current growth in PT facilities and proton treatments for patients worldwide (Diener-West *et al.*, 2001).

1.3 Hypothesis and Research Objectives

Hypothesis:

- There exists a variation in radiation sensitivity between the two different breast cell lines.
- There exist a variation in the radiation sensitivity along the 200 MeV proton beamline.
- There exists a significant increase in the RBE at the distal fall-off (D80% and D40%) of the 200 MeV proton beam relative to the plateau region, thus;

The objective of this study was to explore whether the radiosensitivity to proton irradiation is:

- Cell line dependent, (by biologically evaluation in two different breast cancer cell lines, MCF7 and MCF10A)
- Differs at different positions along the SOBP (and hence the effect on RBE)

1.4 Rationale for this Study

There are a few studies which determined the RBE in the distal end of the SOBP that were previously performed at iThemba LABS in collaboration with Université catholique de Louvain (UCL) in Belgium (Gueulette *et al.*, 1997; Slabbert *et al.*, 2015), and all showed a relative increase in the distal end of the SOBP. The project done in 1997 however, used intestinal crypt cells in mice and focussed on various position in the SOBP and not at the distal fall-off, while the study in 2015 only focussed on the very end of the SOBP. Neither of these studies done at iThemba LABS was devoted to breast cell lines nor the possibility of increased radiosensitivity at the distal fall-off of the proton beam.

CHAPTER 2: LITERATURE REVIEW

***Overview**: Related information about photon radiation therapy and radiobiology are discussed during this opening section and how proton therapy plays a role in the treatment of breast cancer. This will include latest photon radiation and current alleged shortcomings. Radiobiology studies done with the use of proton therapy either in vitro, in vivo or treatment planning studies will be reviewed in this chapter.*

2.1 Radiation Therapy for Breast Cancer

2.1.1 Photon Therapy

The standard care to patients with early breast cancer is breast conserving therapy (BCT), this refers to breast conserving surgery (BCS) followed by moderate-dose RT to eradicate any microscopic residual disease (Litière *et al.*, 2018). Almost 60% of patients will receive radiation therapy for a more advanced stage of breast cancer (Miller *et al.*, 2016).

Historically, radiation therapy increased the long-term mortality of heart disease and secondary lung cancer (Darby *et al.*, 2005; Hooning *et al.*, 2007). Toxicity to normal tissue has been decreased due to improvements in engineering and computing in the delivering of radiation. One of the advances made in the treatment of breast cancer in the early 1990's was intensity-modulated radiotherapy (IMRT) (Nissen and Appelt, 2013), which allows for a computer-controlled multi-leave collimators (MLC) to create a desired dose inside the breast targeted area (Haciislamoglu *et al.*, 2016; Buwenge *et al.*, 2017; Chan, Tan and Tang, 2017). Although the radiation delivery was improved (Garibaldi *et al.*, 2017), the negative effect was the increase in secondary malignancies due to the increased exposure of healthy tissue to low doses of radiation (Prochazka *et al.*, 2002; Kaufman *et al.*, 2008). (Sakthivel *et al.*, 2017) Different forms of IMRT have subsequently been developed to decrease the integral dose, like the volumetric modulated arc therapy (VMAT) to modulate or control the intensity of the radiation beam in multiple small volumes, in order to obtain a more conform 3D shape of the tumour (Buwenge *et al.*, 2017). However, the integral dose calculated still showed a theoretically increased risk of secondary cancers and was not pursued further (Tyran *et al.*, 2015). The dose outside of the targeted area appeared to be inevitable to avoid thus advances to have a steeper dose gradient outside the targeted evolved in the form of breast stereotactic radiotherapy (BSRT) was developed (Yu *et al.*, 2013). Yet, this technique seemed only beneficial to early stage breast cancer patients, as this (Haas *et al.*, 2015; Zagar, Cardinale and Marks, 2016; Kaidar-Person *et al.*, 2017) method is highly dependent on in-room imaging and can be a more expensive treatment option (Pan *et al.*, 2011; Lievens *et al.*, 2015).

The major side-effects when radiating breast cancer patients is the development of secondary lung cancer and/or ischemic heart disease (Clarke *et al.*, 2005; Darby *et al.*, 2005; Early Breast Cancer Trialists Collaborative Group (EBCTCG), 2005; Taylor *et al.*, 2007; Jacob *et al.*, 2016; Corradini, Ballhausen, *et al.*, 2018). Reducing the total radiation dose to less than 5 Gy reduces long-term cardiovascular events but this should be done in such a manner that tumour control is not sacrificed (Nilsson *et al.*, 2012; Mailhot Vega *et al.*, 2016). Most modern techniques, such as respiratory-gated radiotherapy in deep-inspiration breath-hold (DIBH) or volumetric-modulated arc radiotherapy (VMAT) does improve local control and breast specific survival (Fisher *et al.*, 2002; Veronesi *et al.*, 2002; Corradini, Niyazi, *et al.*, 2018) while long term complications remain a significant concern (Brenner *et al.*, 2014). It could take several months to years for heart disease to develop after radiation therapy (Yusuf *et al.*, 2017). The post treatment late side effects are increased (Bradshaw *et al.*, 2016), signifying that the dose to the heart is significantly high (Jacobson *et al.*, 2013; Hong *et al.*, 2017) and could lead to an increase in mortality (Cheng *et al.*, 2017). Further research is needed to determine the optimal dose volume parameters to prevent cardiac disease and death (Frandsen *et al.*, 2015). It has been suggested that with improvements in radiation delivery methods; the survival rate could increase radically (Narod, Iqbal and Miller, 2015).

2.1.2 Proton Therapy

The comparison of PT with conventional photon RT, allows for a theoretic improvement in acute and late toxicity. This is the result of the sharp dose fall-off after the radiation target is reached, decreasing the exit dose to normal tissues (Foote *et al.*, 2012). After a short build-up region, conventional radiation shows an exponentially decreasing energy deposition with increasing depth in tissue. In contrast, protons demonstrate an increasing energy deposition with penetration distance leading to a maximum (the “Bragg peak”) near the end of range of the proton beam as seen previously in Figure 1.1.

Current PT techniques are comprised of two main types: passive scattering proton therapy (PPT) and pencil beam scanning proton therapy (PBS). In PPT, a range modulator is used to spread out the narrow pencil beam produced by a proton accelerator, resulting in a spread-out Bragg peak. In principle, the SOBP dose distribution is created by adding the contributions of individually modulated pristine Bragg peaks. Scattering foils are then used to obtain a field aperture with a homogeneous particle flux sufficiently large for RT applications (Fontenot, Newhauser and Titt, 2005). Whereas, in PBS deflecting magnets and energy modulation of the pristine proton beam are used to apply lateral and longitudinal modulation of the Bragg peak beam spots (Lomax *et al.*, 2004). This method can be used to apply intensity-modulated proton therapy (IMPT) in which the energy and intensity of the proton pencil beams are varied. In analogy with photon IMRT, this technology delivers non-uniform dose distributions from each treatment beam which are combined to the desired (uniform) dose distribution in the target volume. Thereby, the dose conformity and normal tissue sparing is further increased. IMPT is an improvement on IMRT with dose modulation along the beam axis as well as lateral, in field, dose modulation enhanced (Kozak *et al.*, 2006).

Studies conducted in the mid 2000’s for breast cancer patients have shown that the PT dose distribution is far superior to other photon therapy techniques. For a similar tumour radiation dose coverage the with heart doses was 19.4% (Tomotherapy technique), 3.1% (3D conformal technique), and 4.0% (IMRT technique) to 0.0% for PT based on a total prescribed dose of 30 Gy. It should be noted that this was a computational analysis and not a clinical investigation. Several studies applied a similar method (Cuaron, MacDonald and Cahlon, 2016) and showed much lower PT doses to the heart from 0% (Xu *et al.*, 2014), 0.1% (Mast *et al.*, 2014), 1.0% (Bradley *et al.*, 2016) and 1.6% (MacDonald, Jimenez, *et al.*, 2013; MacDonald) of the prescribed total dose compared to photons dose heart coverage ranging between 3.5% to as high as 21% of the prescribed total dose in the respective studies.

A 2013 study was conducted with 12 breast cancer patients to assess acute skin reactions for PT (MacDonald, Patel, *et al.*, 2013), where the entrance dose to the skin was found to be increased based on the SOBP range (Gottschalk, 2003; Kooy *et al.*, 2003). Grade 1 skin toxicity (faint or dull redness of the skin) appeared within the first 4 weeks in 8 patients but was still favourable compared to photons; this was later confirmed by a similar investigation in 2015 (Cuaron *et al.*, 2015). Both these studies mention that late complications (especially heart toxicity) could not be assessed due to the lack of additional patient follow-up. Since cardiac toxicity is a major concern when treating breast cancer (Hong *et al.*, 2017), and based on the proximity to the breast, the variation in RBE in distal edge of the proton beam could have an impact on possible late toxicity to the heart (Wang, 2015).

2.2 LET Increase at the Distal Edge of the Proton Beam

PT is recommended for tumours with critical structures in very close proximity to the targeted area (Dennis *et al.*, 2013). Although the dose fall-off close to critical structures shows signs of increased LET (Titt *et al.*, 2017), the range of the SOBP to cover the targeted area could have a negative effect on the normal tissue. This was further emphasised by Gensheimer *et al* for a improvement in treatment planning practice to reflect the increase in LET at the distal region (Gensheimer *et al.*, 2010).

Furthermore, it was shown that for a 10 cm SOBP the distal fall-off range was measured to be 6 mm (Nichiporov, Hsi and Farr, 2012), which could be significant when it comes to breast treatment (larger treatment ranges) and where the heart is in such close proximity to the breast. Therefore, greater concerns arose when increasing the SOBP resulting in a more gradual dose-fall-off and spreading over a bigger range than expected (Elmekawy *et al.*, 2014), furthermore, resulting in an increase in RBE and range extension (Paganetti, 2003; Wilkens and Oelfke, 2004).

2.3 Radiobiology Concerns

Relative biological effectiveness (RBE) for proton therapy is considered a complex function depending on various physical and biological parameters such as radiation dose, LET, dose rate, dose fractionation, cell type as well as biological endpoint, (Paganetti, 2014). Despite studies showing considerable uncertainties in proton RBE values, the assumption of a fixed RBE of 1.1 is still applied in clinical practice. This RBE increase translates an extension of the biological-effective range of the treatment field by up to a few millimetres beyond the distal edge of the target volume and may result in a biologically effective dose distribution different from that approved on treatment plans. This may contribute to unexpected toxicities and could lead to failure to control the disease (Mohan *et al.*, 2017).

An *in vivo* study done in 2017 by Sørensen and co-workers indicated that for a clinical proton, using a scanning beam, the RBE for early damage (in mice models) increases due to an increase in LET towards the distal edge of the SOBP and the distal fall-off (Sørensen *et al.*, 2017). The biological endpoint chosen was to assess skin damage of the foot of the mice using a mouse foot scoring system. An increased RBE was found in the distal edge of the 3 cm SOBP and the first part of the distal dose drop-off. It has also been reported that RBE at the Bragg peak may be between 30 and 40% higher than the entrance plateau dose (Mohan *et al.*, 2017). From the doses used, it was not clear whether the RBE does change in different points in the dose fall-off as the RBE is not only dependent on the LET but also on the dose and tissue type used (Alexandru and Iuliana, 2012; Tommasino and Durante, 2015; Jones, 2016).

This increased RBE in the Bragg peak was emphasised when human fibroblast cells were irradiated with 219.65 MeV protons. The results indicated a significant increase in cell killing RBE when smaller dose per fraction were used (Marshall *et al.*, 2016). RBE increased from 1.17 to 1.24 in the Bragg peak region for proton dose fractionation from 3.6 Gy to 0.8 Gy respectively. This suggested that new considerations should be introduced to the adoption of modified fractionation schemes (Hosseini, Jia and Ebrahimi-Loushab, 2017).

In summary, it has been shown that *in vitro* studies confirmed an increase in dose-averaged corresponds to an increase in RBE compared to 6 MV photons with depth in the SOBP from 1.15 in the centre of the SOBP, to about 1.35 in the distal edge and 1.7 in the distal fall-off region (Ilicic, Combs and Schmid, 2018; Underwood and Paganetti, 2018). Several studies reported variation in RBE for different proton beam energies (Calugaru *et al.*, 2011; Jones, McMahon and Prise, 2018), with different biological endpoints (Ando *et al.*, 2001; Green *et al.*, 2001; Friedland *et al.*, 2003; Friedrich *et al.*, 2012; Ilicic, Combs and Schmid, 2018) and tissue types (Ando *et al.*, 2001; Calugaru *et al.*, 2011; Britten *et al.*, 2013; Hojo *et al.*, 2017).

Confirmation of RBE variation for protons can be achieved with different methods, (Paganetti et al., 2002), such as sequential magnetic resonance imaging (MRI) to detect changes in anatomy after 77 to 115 weeks post irradiation (Benczik et al., 2002). This method was used to determine the RBE (relative to 6 MV photons) of an epithermal neutron beam on the brains of dogs by establishing a dose effect relationship with the images of, post and prior radiation. These findings concluded RBE values of 1.2 - 1.3 for protons from nitrogen capture and 3.5 - 4.0 for protons from fast neutrons relative to a 6 MV photon radiation.

A recent clinical study by Peeler et al, was done to express the variable proton RBE in 34 paediatric patients treated for ependymoma (Peeler et al., 2016). They concluded that a LET variation was shown in the MRI done 1 to 8 months after radiation and was comparable to results predicted from Monte Carlo calculations and thus an indication of variation in RBE.

2.4 Cell Type and Radiobiological Endpoints Relationship with RBE

Correlated damage of the DNA due to radiation (especially for high LET radiation) occur more often within a cell and becomes more difficult for the cell to repair itself (Goodhead, 1999). Radioresistant cells have a higher repair capacity while radiosensitive cells have a lower repair capacity (Weyrather *et al.*, 1999). Variations in LET and RBE within a proton therapy beam, perceptibly cell repair also fluctuate (Mohan *et al.*, 2017). Different studies have found varying values for proton RBE, when various murine tissues were found to have RBE values ranging between 1.09 and 1.32 (Urano *et al.*, 1984), to 2014 when it was reported that hypopharyngeal squamous cell carcinoma cells also from mice resulted in RBE values of 1.1 - 1.2 relative to 6 MV photons. Early studies show a close RBE value compared to photons, whereas, cancer stem cells presented an extra resistance to photon therapy compared to proton therapy (Fu *et al.*, 2012; Zhang *et al.*, 2013). Recent literature indicates that highly radiosensitive tumours have the lowest RBEs, often below 1.1 while radioresistant tumours have higher RBE's (Jones, 2017).

Various radiobiological endpoints can provide different perceptions into cell RBE such as chromosome aberrations, foci formation or even apoptosis (Paganetti, 2014). Choosing a cell survival endpoint might not give the true representation of RBE for unrepaired or misrepaired damage that can transfer changes to the descendent cell (Bentzen, 2006). It has been shown that the increase in RBE is less steep for double strand breaks (DSB) than for cell survival (Barendsen, 1979). A more recent radiobiological endpoint that is often used to study DNA DSB induction and repair is the gamma-H2AX foci assay (Kuo and Yang, 2008), although in human salivary gland tumour cells did not show an increase in a function of depth in a SOBP (Baek *et al.*, 2008) indicating an increase in LET in depth does not indicate an increase in DSB, which would then cause an increase of RBE (Mohan *et al.*, 2017). However, another study where human skin fibroblast underwent proton irradiation an increase in complex DNA damage was seen in the distal edge (Chaudhary *et al.*, 2016).

A correlation between foci size and cell survival does show an improved correlation with radiation effectiveness compared to the number of foci 6 hours after radiation (Ibanez *et al.*, 2009). Chromosome aberrations or improper repair of DNA damage is another radiobiological endpoint use to determine RBE (Wu *et al.*, 1997). Studies using this biological endpoint resulted in very different RBE values for PT (Todorov *et al.*, 1972; Schmid, Schraube and Bauchinger, 1998; Mognato *et al.*, 2003). Radiosensitivity studies using the Cytokinesis-Block Micronucleus (CBMN) assay is one of the most common radiobiological endpoints used to assess a human cell's sensitivity (Guogytė *et al.*, 2017). The micronuclei represents a loss of genetic material that fail to attached to the mitotic spindle (Paganetti, 2014) and can be used to calculate RBE (Joksic *et al.*, 2000; Sgura *et al.*, 2000; Green *et al.*, 2001; Yang, Anzenberg and Held, 2007; Antoccia *et al.*, 2009).

2.5 Radiosensitivity and RBE Relationship

Cellular radiosensitivity can provide important insights into identifying the different responses of both tumour and normal tissues in PT (Zhao *et al.*, 2017). Although PT does have some physical benefits over photon radiation, the variation in RBE at the distal part of the beam adds to the radiobiological uncertainty and cellular responses (Tommasino and Durante, 2015). An accurate RBE to determine the cellular response of tissues is therefore critical to determine radiosensitivity and vice versa for PT (Paganetti *et al.*, 2002). However, slight variations in RBE values would not be as clinical significant compared to individual radiosensitivity variations and therefore the latter must be as accurate as possible for radiation therapy (Hawkins, 2009). Although a strong positive correlation does exist

between RBE and radiosensitivity the relationship still needs to be accurately quantified (Zhao *et al.*, 2017).

It might be impossible to measure all RBE values for every clinically relevant set of conditions but cellular radiosensitivity can assist with the understanding of interactions between radiation and tissues (Scholz and Elsässer, 2007; Friedrich, 2016).

CHAPTER 3: MATERIALS AND METHODS

***Overview**: Related information about proton beam calibration radiation procedure, micronuclei scoring followed by data analysis.*

3.1 Outline of Research Materials and Methods

The experimental technique that was followed, was a quantitative approach and is a well-established and widely used method in the field of radiation biology (Fenech, 2007). The radiosensitivity of MCF7 and MCF10A breast cell lines was assessed *in vitro*, by means of the cytokinesis-block micronucleus (CBMN) assay, after being irradiated at six different positions using a clinical 200MeV proton beam.

3.1.1 Physical Phase

The cell lines were irradiated at room temperature with 200 MeV protons produced at NRF iThemba LABS in a Perspex phantom (designed at NRF iThemba LABS). A monolayer of cells was irradiated in a 25 cm2 culture flask at different water equivalent depths in a 5cm SOBP. Absolute dose measurements were performed by using the Markus Chamber, a classic plane-parallel dosimetry chamber.

3.1.2 Chemical Phase

Immediately after irradiation, cells were allowed to complete one nuclear division, with cytokinesis blocked by the addition of 7.5 µL Cytochalasin B per 5 mL medium concentration, resulting in binucleated (BN) cells. The cells were then manually scored by assessing DNA damage in the form of micronuclei (MN), using the Zeiss Axio Score A.1 fluorescent microscope. MN were formed in the cytoplasm when whole chromosomes or chromosomal fragments failed to engage with the mitotic spindle, and were not incorporated into the daughter nuclei subsequent to cell division (Norppa and Falck, 2003). The results of mis-repaired or non-repaired DNA damage derived from the MN assay was then used as a biological marker to assess radiosensitivity and to calculate RBE values at different positions along the SOBP relative to the entrance plateau region.

3.2 Radiation Physics and Dosimetry

The 200-MeV clinical proton beam was produced at NRF iThemba LABS using a separated-sector cyclotron. The beam had a fixed horizontal direction and was laterally spread and flattened using a double-scattered/occluding-ring system (Slabbert et al., 2015). A schematic layout in Figure 3.1 shows the beam delivery system.

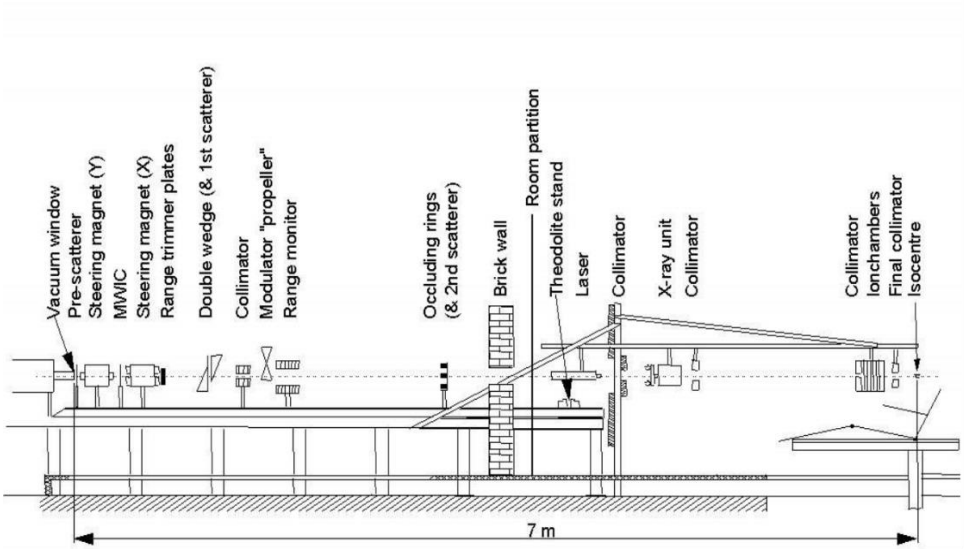

Figure 3.1: A schematic layout of the clinical proton beam delivery system used at iThemba LABS (Slabbert et al., 2015).

The beam was controlled by two feedback systems using both the 'X' and 'Y' steering magnets. The first feedback system used a multi-wire ionisation chamber (MWIC) that monitors the beam position in both the 'X' and 'Y' planes perpendicular to the beam direction, thus ensuring that the beam is correctly aligned. The second feedback system, a segmented transmission ion chamber, is located closer to the research samples and monitors the symmetry of the proton beam. The collimators located in the beamline are to reduce scatter radiation (Brenner *et al.*, 2009).

During the experiments, an energy of 198.7 MeV was used and normalised to 200MeV by changing the double wedge settings (and range shifter plates) and had a residual range of 23.70 cm in water as illustrated in Figure 3.2.

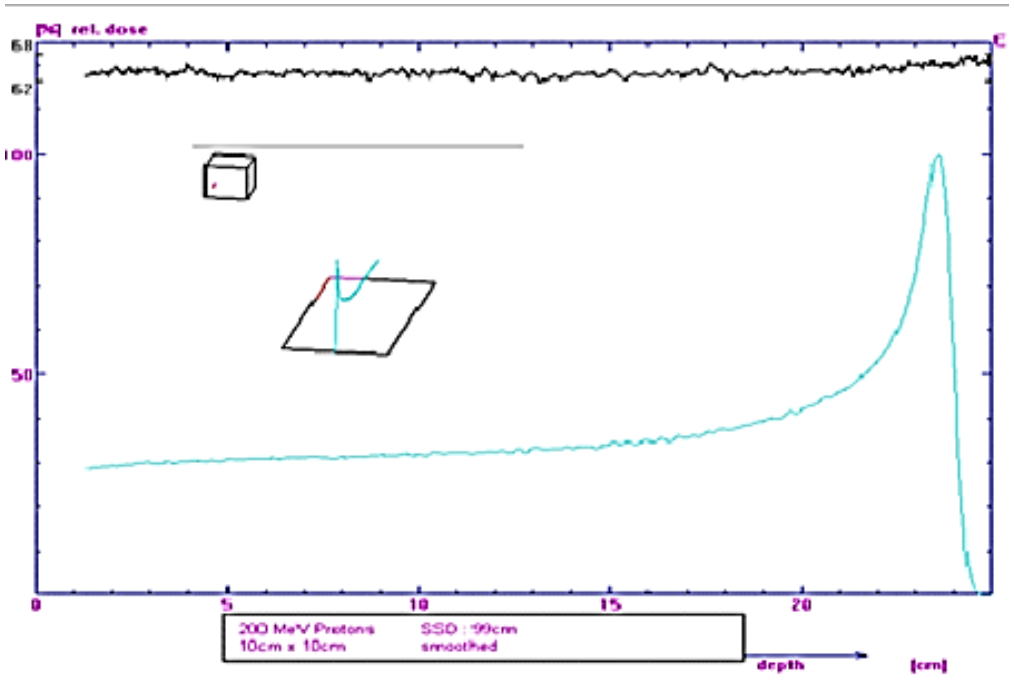

Figure 3.2: Upstream depth dose curve for 10 cm field diameter.
Depth dose curve measured in the water phantom without the modulator propeller in the beam. The range shifter plates where placed upstream of

the range monitor in order to routinely produce a residual range of 24.00 ± 0.03 cm during the quality assurance testing.

These online measurements were checked against a set of depth-dose, perpendicular and transverse scans, (Figures 3.2, 3.3 and 3.4), showing the depth-dose scan, cross-plane as well as in-plane scans respectively in a 3D scanning water phantom.

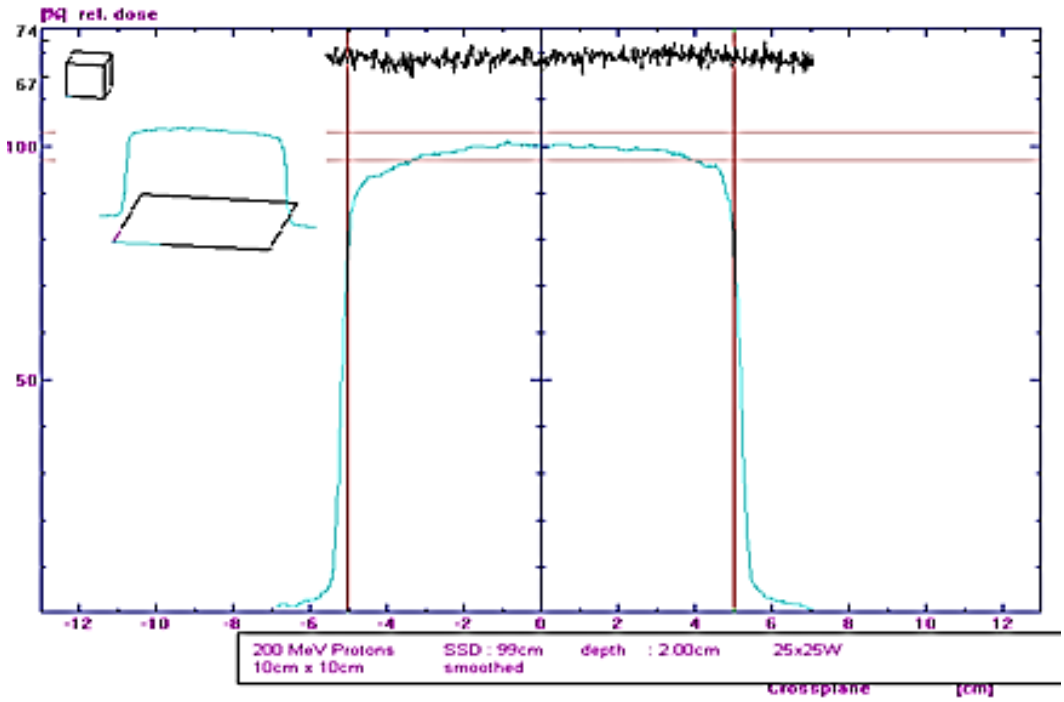

Figure 3.3: Crossplane depth dose curve to check the range of a 10cm field diameter.
Crossplane depth dose curve measured in the water phantom without the modulator propeller in the beam. The range shifter plates were placed upstream of the range monitor in order to routinely produce a residual range of 24.00 ± 0.03 cm during the quality assurance testing.

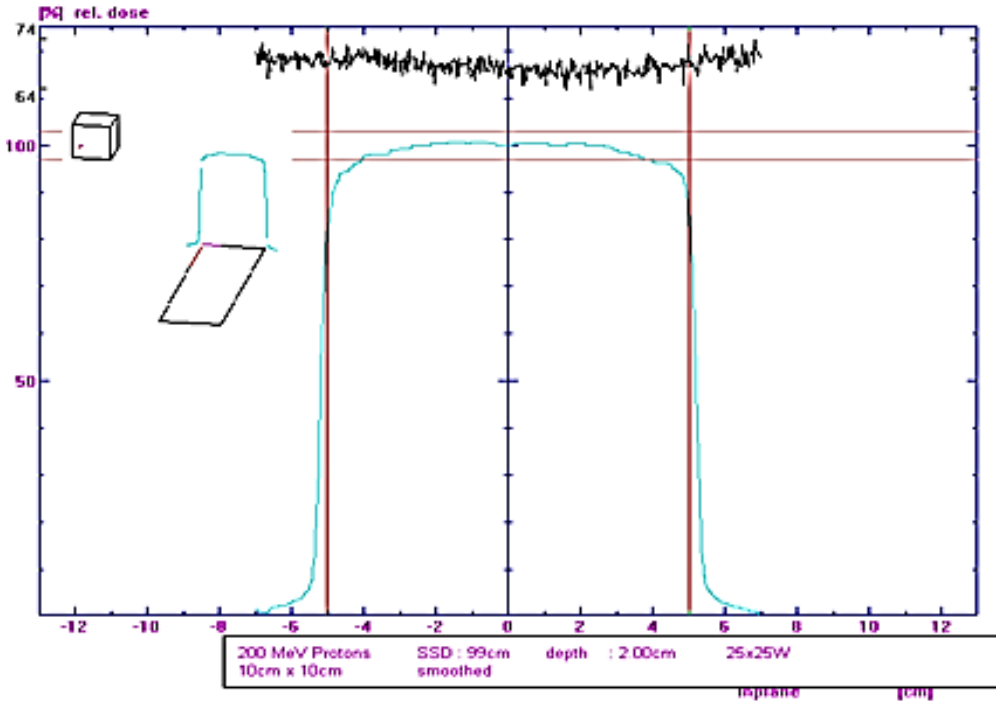

Figure 3.4: Inplane depth dose curve width check for a 10 cm field diameter.
In-plane depth dose curve measured in the water phantom without the modulator propeller in the beam. The range shifter plates were placed upstream of the range monitor in order to routinely produce a residual range of 24.00 ± 0.03 cm during the quality assurance testing

The beam profile was checked by a qualified medical physicist by examining a depth-dose curve and checking that the range, entrance dose, and the full width at half maximum of the Bragg peak were within prescribed limits. The transverse profiles were checked for symmetry and flatness to ensure proper alignment of the beam. The scans were analysed and checked for compliance with set limits.

The Spread-Out Bragg peak (SOBP) of 5 cm was modulated using a rotating stepper-absorber (or a modulator wheel) as shown in Figure 3.1. The beam quality was checked by a set of perpendicular transverse scans and a depth-dose scan in a 3D scanning water phantom as shown in Figure 3.3.

The transverse profiles were checked for symmetry and flatness to ensure that the beam is properly aligned (Figures 3.2, 3.3 and 3.4). A multi-layer Faraday cup and a set of stacked ionisation chambers were used to check the energy and the energy distribution of the beam. Absolute calibration was then done in a water phantom Figure 3.5 as per TRS398. (1 MU = 1 Gy)(Arib, Medjadj and Boudouma, 2006).

The Markus chamber measurements were cross-calibrated against the reference chamber, and different output factors were measured for different depths in Figure 3.5.

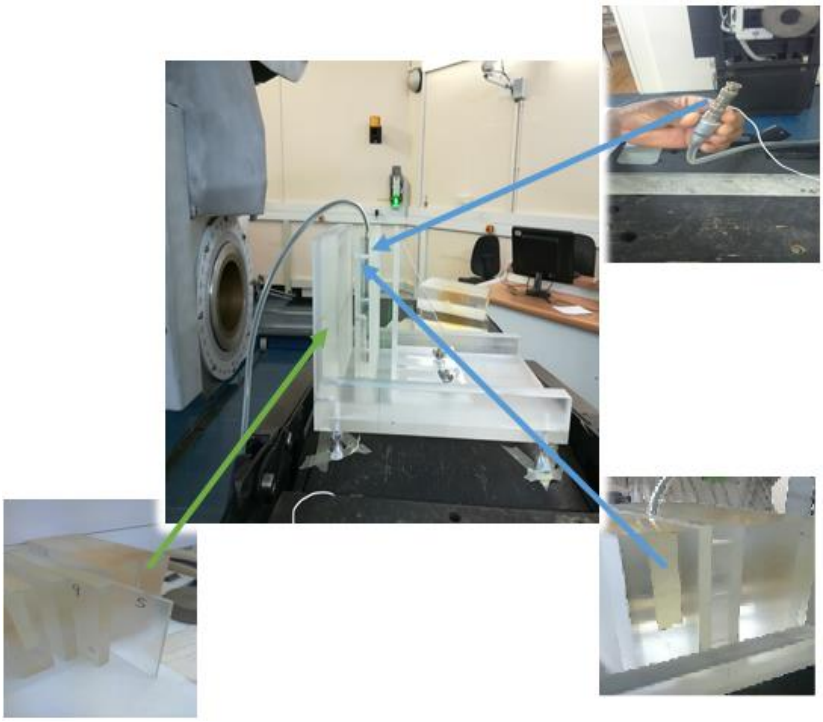

Figure 3.5: Marcus chamber and Perspex thickness used for beam calibrations.

Markus chamber (green arrow) inserted inside the Perspex blocks used to cross calibrate the proton doses at different depths, and different Perspex thickness combinations used (blue arrows) to resemble the different measurement depths. This set-up was used for both the experiment and dosimetry with the jig.

A Perspex phantom was designed and built at iThemba LABS for this experiment allowing for different thicknesses of Perspex plates representative of different water equivalent thicknesses (WET) and to house the cell culture flask as shown in Figures 3.6 and 3.7. The water equivalent thickness for the Perspex plates were calculated as shown in Equation 2 (Zhang and Newhauser, 2009)

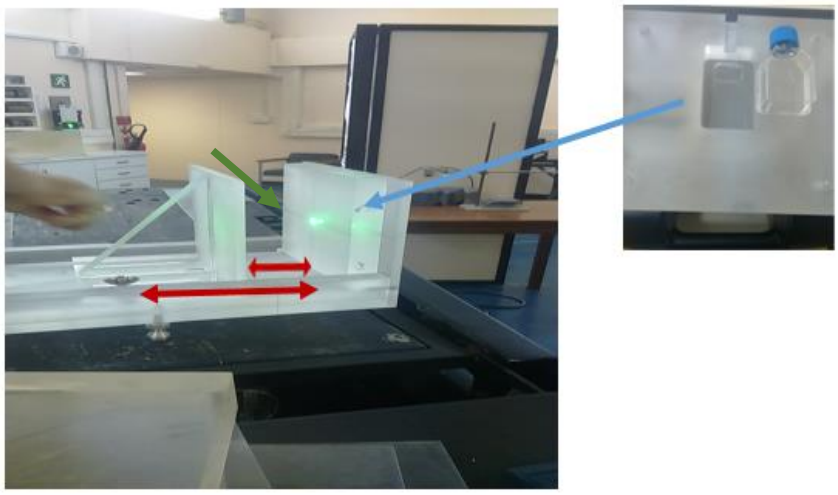

Figure 3.6: Perspex phantom to allow irradiation of a monolayer of cells in a cell culture flask at different depths.

The phantom can be adjusted (red arrows) to accommodate different Perspex plates depending on the depth (based on water equivalent thickness required) within the proton beam. The green arrow indicates different thicknesses of Perspex plate combinations needed to create different depths in the proton beam while the blue arrows indicate the space in a Perspex plate to house the Markus chamber for dosimetry.

Different Perspex blocks were used to obtain the different depths needed, with the water equivalent thickness for the perspex plates were calculated as shown in Equation 2 (Zhang and Newhauser, 2009).

Figure 3.7: Perspex plate housing

A Perspex plate made at iThemba LABS to hold the culture flask with the cell lines for the experiment. The red arrow indicates the space provided to accommodate the culture flask

The general equation for WET is:

Equation 2: The water equivalent thickness equation.

$$t_w = t_m \frac{\rho_m}{\rho_w} \frac{\bar{S}_m}{\bar{S}_w},$$

where *tw* and *tm* are the thicknesses of water and the target material, respectively; *ρw* and *ρm* are the mass densities of water and the material, respectively; and $\bar{S}$m and $\bar{S}$w are the mean values of mass stopping power for material and the water, respectively (Zhang and Newhauser, 2009).

The above equation was applied to determine the different thickness combinations of Perspex plates to produce different depths within the proton beam as indicated in Figure 3.8.

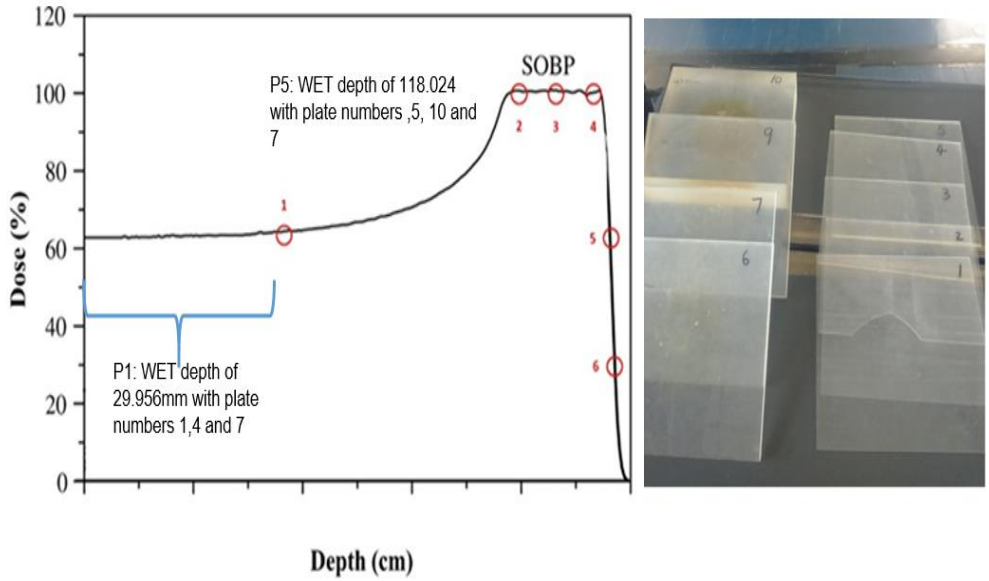

Figure 3.8: Water equivalent thickness application within the proton beam. Different plate combinations indicating the different depths within the proton beam based on the WET calculations.

3.3 Biology Procedure

3.3.1 *In vitro* culturing of the cancerous breast cells lines

Michigan Cancer Foundation-7 (MCF-7) cell lines are human adenocarcinoma breast cancer cell lines with estrogen receptors (ER's) and glucocorticoid receptors (Camarillo *et al.*, 2014). These cells are useful for *in vitro* breast cancer studies. The cell line retains several characteristics of differentiated mammary epithelium cells and are the most common cell line used to study breast cancer (Lee, Oesterreich and Davidson, 2015). The MCF-7 cells were cultured using Dulbecco's Modified Eagle's medium F-12 (DMEM F-12) that contained a higher concentration of amino acids and vitamins, as well as additional supplementary components with 10% Fetal Bovine Serum (FBS) for growth, penicillin (100 µg/L) to prevent bacterial contamination together with streptomycin (100 µg/mL) as antibiotic solution to prevent bacterial contamination in a T25 culture flask.

3.3.2 *In vitro* culturing of the non-malignant breast cells lines

Michigan Cancer Foundation 10A (MCF10A) is a spontaneously immortalised, non-malignant breast cell line obtained from a patient with benign fibrocystic disease (Dawson *et al.*, 1996) and is a non-tumorigenic epithelial cell line. MCF-10A cells were cultured using Dulbecco's Modified Eagle's medium F-12 (DMEM F-12), supplemented with 1% penicillin streptomycin, 5% FBS, 0.5 µg/mL hydrocortisone, 20 ng/mL Epidermal Growth Factor (EGF) and 10 µg/mL insulin (Debnath, Muthuswamy and Brugge, 2003).

Cells were trypsinated from a T75 culture flask and re-suspended in growth medium to ensure enzyme inactivation, counted using haemocytometer and seeded accordingly in a T25 culture flask according to dose and position needed for different parts of the depth dose curve.
All cultures were seeded the day before to allow the cells to settle and attach to the base of the flask.

3.4 Irradiation Procedure

The Perspex phantom designed at NRF iThemba LABS allowed for a positioning accuracy of 0.1 mm. The phantom consisted of two Perspex plates that were specifically designed to hold a flask (Figure 3.7). Additional plates of various thicknesses were interposed in front of the petri-dish in order to obtain different water equivalent depths. Reference dosimetry was carried out with a Markus chamber and irradiations were performed with a 198.5 MeV proton beam generated at NRF iThemba LABS that was degraded to a R50 (half-value depths) range of 120 mm, with a field size of 10 cm x10 cm and a 50 mm SOBP. Cells were then exposed to 0.5, 1.0, 2.0, 3.0 and 4.0 Gy doses for each cell line independently and for each position.

Table 1 summarises the different depths used for both cell lines, expressed as a percentage of the maximum depth dose which was normalised to a reference position in the SOBP plateau at 109.82 mm water equivalent depth in the SOBP (100% or maximum dose position):

Table 1. Different WET depths for each position and percentage depth dose.

Position	WET Depth (mm)	% Dose
1	29.96	74.88
2	74.86	102.59
3	94.97	101.10
4	109.82	100.00
5	118.02	83.44
6	120.98	39.76

3.5 Post-irradiation Cell Processing

Immediately after irradiation, 7.5 µL Cytochalasin B per 5 mL medium (concentration 2.25 µL/mL) was added. The cultures were incubated for 48 hours to inhibit cytoplasmic division and to enable micronuclei (MNi) formation after anaphase division. Thereafter, the cells were trypsinated and harvested by washing them with 5mL of the hypotonic solution KCl (pH 7.4). The cells were spun down via centrifugation, the supernatant removed and the cell pellet washed with 5mL cold methanol/acetic acid/Ringer's solution (10:1:11) solution to fix the cells and maintain structural integrity. The samples were then fixed with methanol/ acetic acid (10:1) solution and slides were prepared with 40 µL of the fixed cell pellet. Once dried, the slides were stained with Acridine Orange and MNi were manually scored with a Zeiss fluorescent microscope (Figure 3.9).

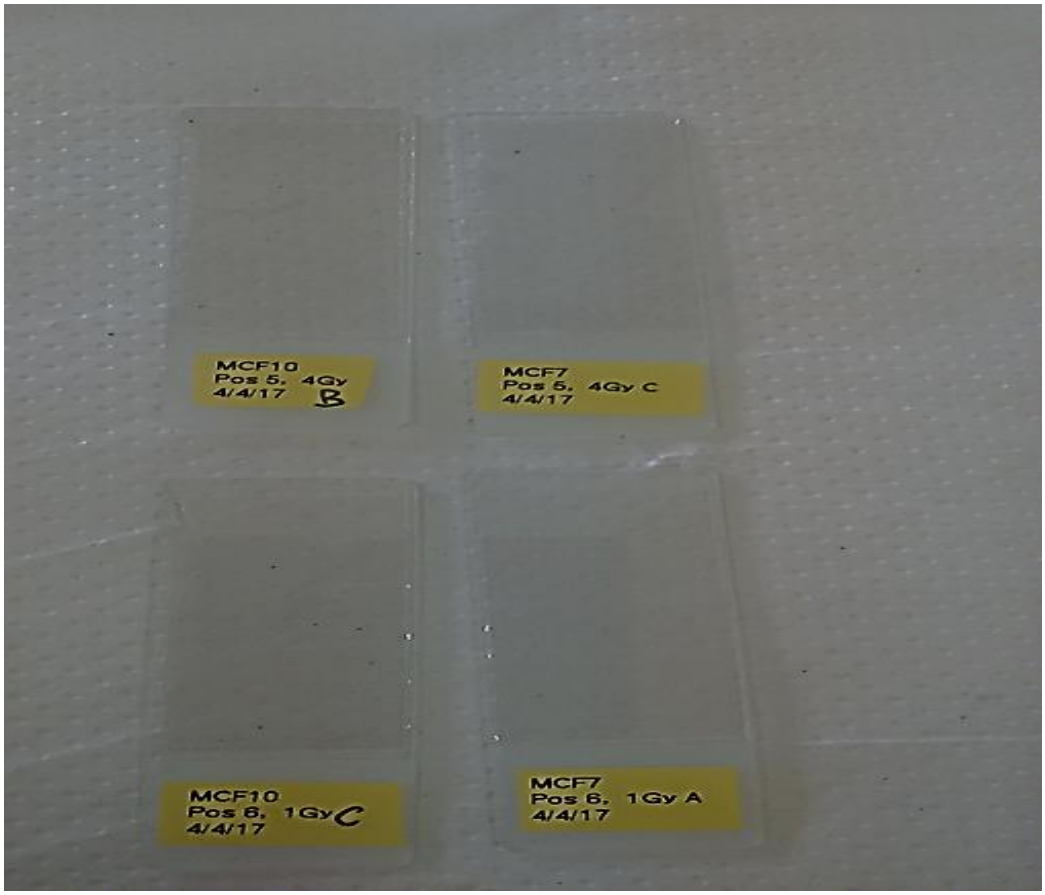

Figure 3.9: Stained slides with coverslips and labels.
Each slide was labelled to indicate the cell line, Bragg peak position, dose, date and whether it is sample A, B or C since slides were made in triplicate.

3.6 Scoring

Following the guidelines described by Vandersickel (Vandersickel *et al.*, 2010), scoring of 500 binucleated cells (BNCs) were manually scored per slide was done manually using an inverted fluorescence microscope (Zeiss) by using the fluorescein isothiocyanate (FITC) filter. The number of MNi was captured within these BNCs to ensure that the chromosomal damage that had occurred due to the proton radiation exposure was captured properly (as shown in Figure 3.10). For each condition (cell line, dose point and position in the proton depth-dose curve), at least 1500 BNCs were manually evaluated over three slides.

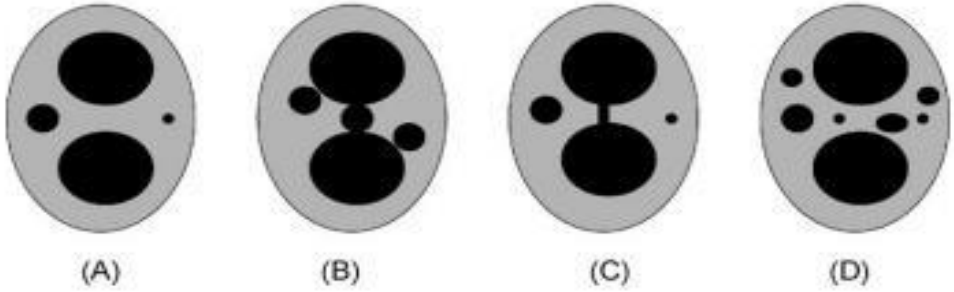

Figure 3.10: The characteristic appearance and relative size of MNi in BNCs.
BNC with two MNi (A) and containing viable MNi varying in sizes between 1/3 and 1/9 of the main nuclei. (B) BNC with three MNi touching, but not overlapping the main nuclei. (C) A BNC with nucleoplasmic bridge between main nuclei and two MNi. (D) A BNC with six MNi varying in sizes (Fenech *et al.*, 2003).

3.7 Bromodeoxyuridine (BrdU) and flow cytometric analysis

As radiosensitivity varies between cell cycle stages, cell cycle kinetics parameters could predict radiosensitivity, especially as cells are more radioresistant in the S-phase (Theron *et al.*, 1997). Bromodeoxyuridine (BrdU) incorporation can be used to quantify the number of cells that are in S-phase in the time period that BrdU is available. The immunofluorescent staining of incorporated BrdU and flow cytometric analysis provide a high-resolution technique to determine the frequency and nature of individual cells that have synthesised DNA during the S-phase stage. The process was done using a FITC BrdU Flow Kit (protocol was supplied). BrdU (an analogue of the DNA precursor thymidine) is incorporated into newly synthesised DNA by cells entering and progressing through the S-phase (DNA synthesis) of the cell cycle. The incorporated BrdU is stained with specific anti-BrdU fluorescent antibodies. The levels of cell-associated BrdU, stained with a dye that binds to DNA such as 7-amino-actinomycin D (7-AAD), are then measured by flow cytometry. With this combination, two-colour flow cytometric analysis permits the enumeration and characterization of cells that are actively synthesizing DNA (BrdU incorporation) in terms of their cell cycle position as shown in Figure 3.11. Each cycle phase was measured as a percentage in terms of the time.

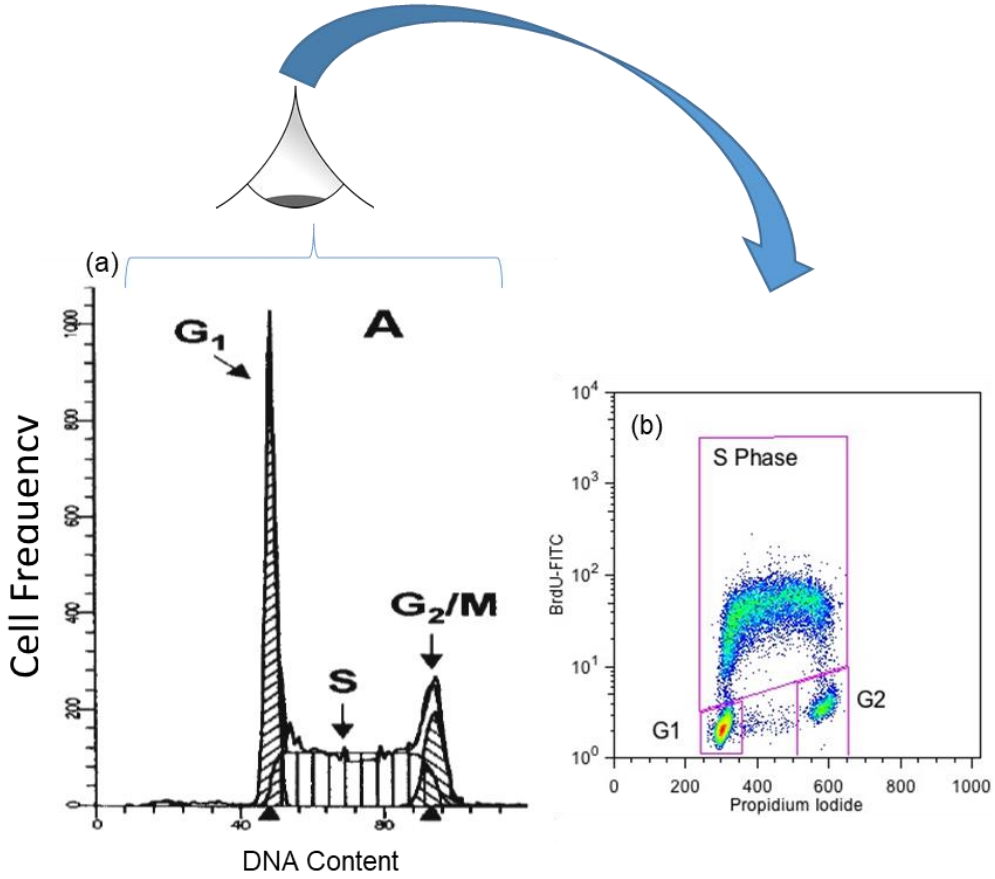

Figure 3.11: DNA content histogram and BrdU measured for the breast MCF-7cell line.

The cell cycle (a) indicating the DNA content during each phase of the cell cycle (Rabinovitch, 1994) and (b) the levels of cell-associated BrdU measured by flow cytometry.

3.8 Data Analysis

The scored MNi were entered into a Microsoft Excel spreadsheet and the mean with standard deviations calculated. Significance testing was done using a student paired T-test. The spreadsheet was then loaded on GraphPad Prism 5 software and non-linear regression analysis was performed. The average number of MNi per dose point and cell line were per plotted and dose-response curves were fitted by using a linear-quadratic (LQ) model, as clarified in Equation 3.

The LQ formulation is often used to model biological response to radiation. For instance, when applied to cell survival studies the surviving fraction (SF) is generally expressed as shown in equation 3 (van Leeuwen *et al.*, 2018).

Equation 3: The linear aquatic equation.

$$E = \alpha D + \beta D^2 + c$$

Where E is the number of micronuclei observed in 1000 binucleated cells, c the background frequency, α the initial slope of the curve and β the bending component of the same curve of each absorbed dose in Gy (D) response curve (Martinez-Planell, Lopez Torres and Robles Hernandez, 2015).

3.8 95% Confidence Ellipse Results

A program was developed on Matlab platform to calculate the 95% confidence ellipse for the co-variance parameters α and β that describes the dose response curve for the average number of radiation induced MN per 1000 BN cells. The program is based on the technique used by Slabbert *et al*. (Slabbert et al., 1989).

CHAPTER 4: RESULTS

***Overview**: Micronucleus assay results together with iso-effective doses calculated are displayed in the first part of this chapter followed by the calculated RBE values with reference to the entrance plateau region for each different positions in the Bragg peak.*

4.1 Micronuclei Assay results

The MNi were counted within BNCs to assess any possible damage enhancement that has occurred will be observed as acentric fragments. The loss of cells during culturing, is not taken into account.. MNi scored for the control samples for MCF-7 and MCF-10A cell lines were 13.33 ± 4.16 and 26.67 ± 8.08 respectively. Figure 4.1 shows the radiation-induced chromosomal damage after irradiation with the reference radiation (entrance plateau) used in this study. With Figure 4.2 and Figure 4.3 showing Acridine Orange (AO) stained MCF-7 and MCF-10A cells exposed to 4 Gy protons at the position deepest in the distal edge (WET depth of 120.975mm - Position 6).

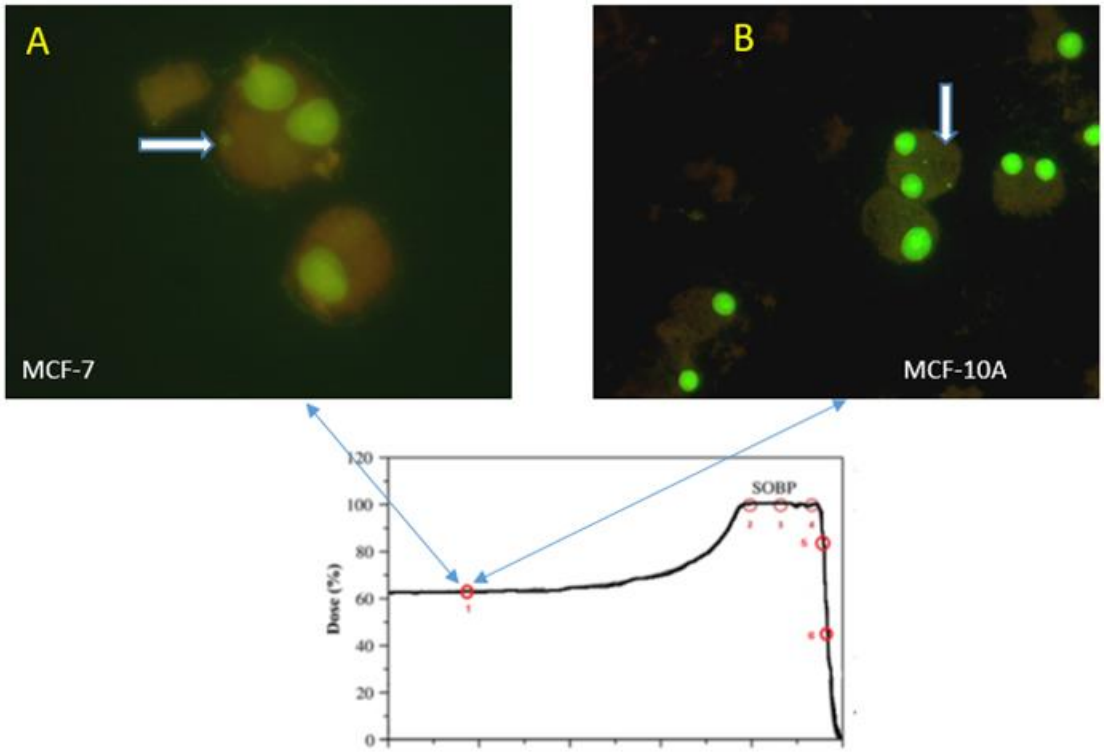

Figure 4.1: Acridine orange (AO) stained MCF-7 and MCF-10A cells exposed to 0.5 Gy protons at the entrance plateau position (Position 1).
Wherein (A) illustrates one micronucleus (MNi) in one BNC for the MCF-7 cells and, (B) two (MNi) in a BNC as well as a BNC for the MCF-10A cells, both (A) and (B) were irradiated at position 1 as indicated above.

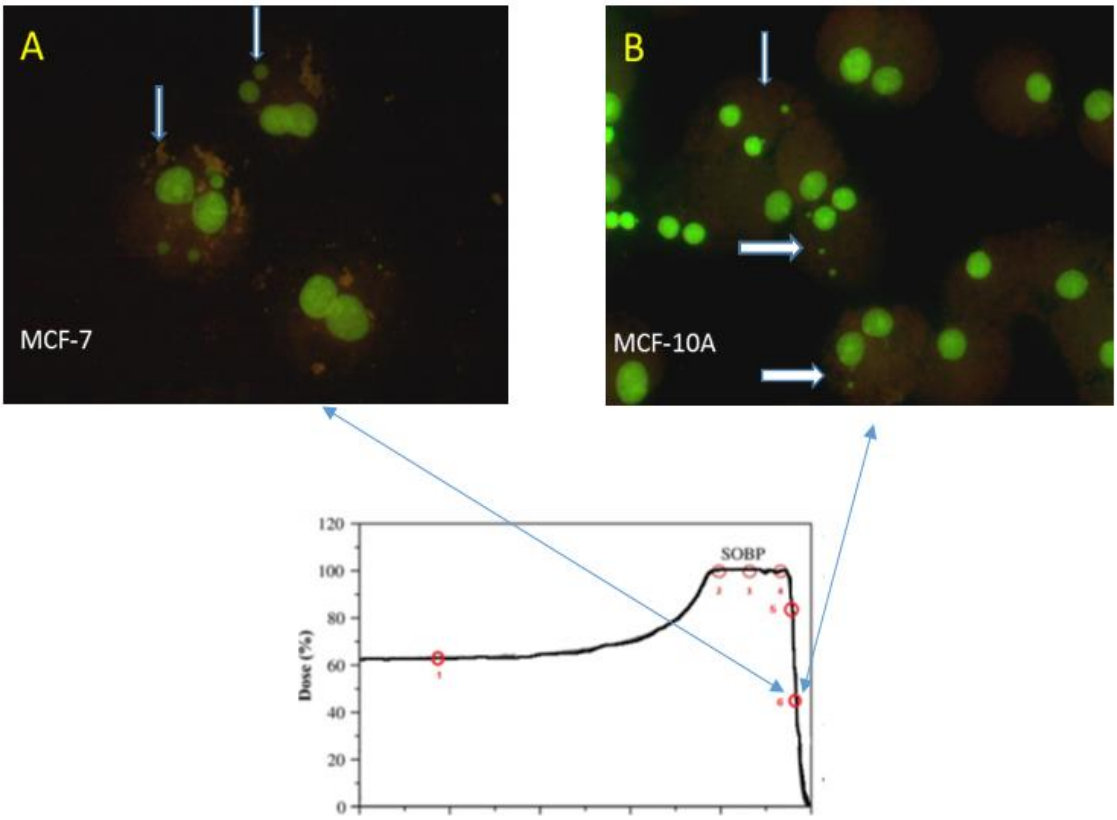

Figure 4.2: MCF-7 and MCF10A cells after CBMN assay post 4Gy protons in the distal fall-off.
Wherein (A) illustrates three BNC and two having 4 MNi and two MNi respectively for the MCF-7 cells and, (B) several BNC two BNC having two MNi and one have three MNi respectively for the MCF-10A cells, both (A) and (B) were irradiated at position 6 as indicated above.

The total number of MNi after deducting the background MNi scored without irradiation (the control group) of the MNi for each radiation dose given at the entrance plateau region is presented in Figure 4.3.

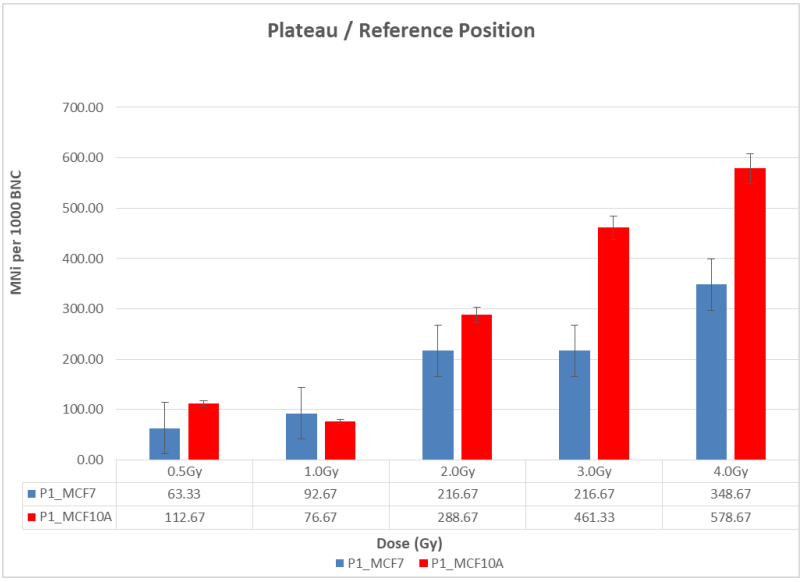

Figure 4.3: MNi scored per 1000 Bi-nucleated cells for both MCF-7 and MCF-10A cells at the reference position.

The results in the plateau region showed an increase in MNi for the normal breast cell line (MCF-10A) compared to the cancerous cell line (MCF-7), with $p = 0.027$, $p = 0.046$ respectively, pointing to a difference in radiosensitivity. This indicates that the cancerous cells were more radioresistant compared to the normal breast cell line in this part of the proton beam.

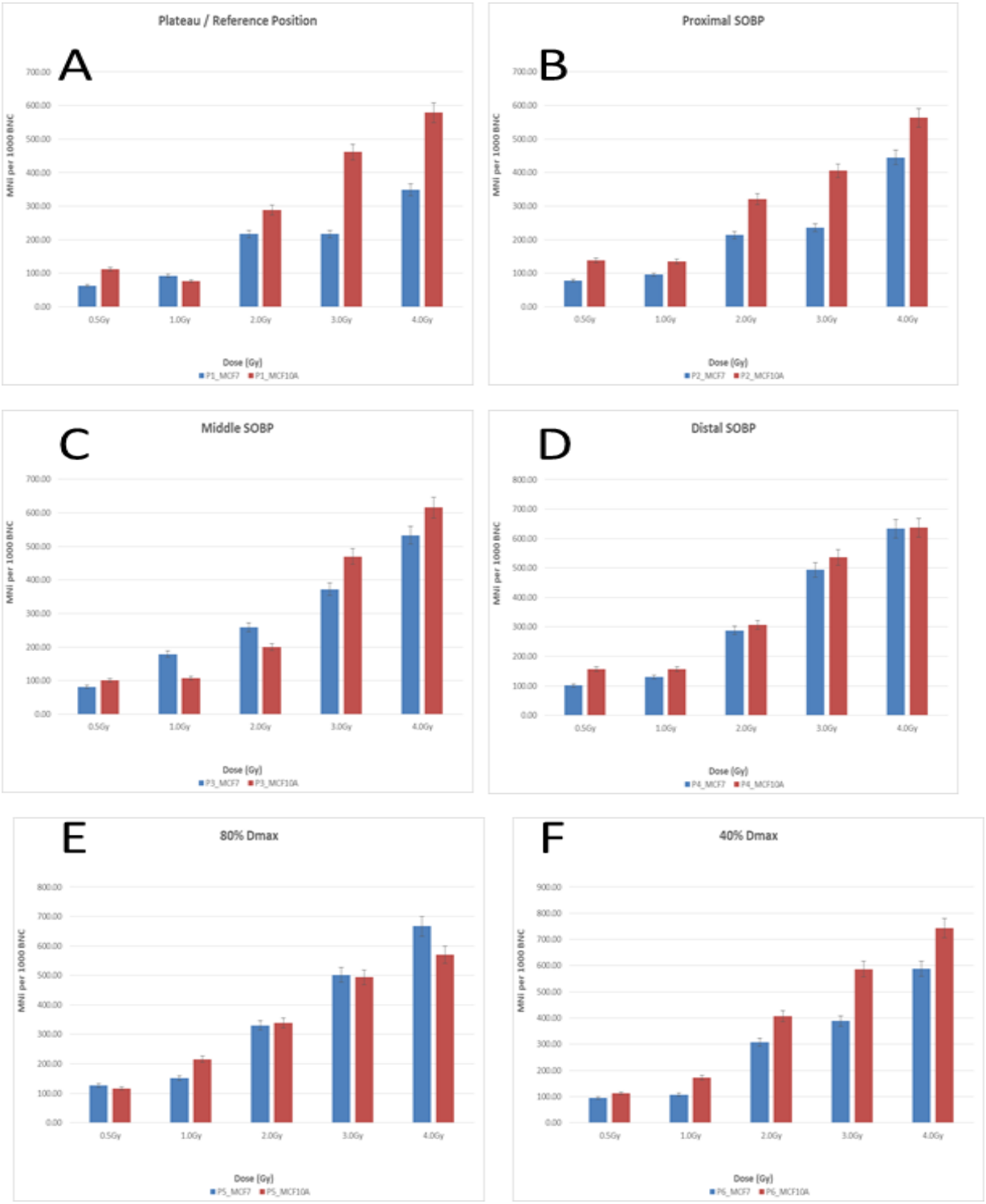

Figure 4.4: Average number of MNi scored for both breast cell lines after irradiation with different proton doses.
Graphs (A) to (F) illustrate the number of MNi at the different positions of the proton beam.

Figure 4.4 shows the average MNi scored for each proton dose given and in each position for both breast cell lines.

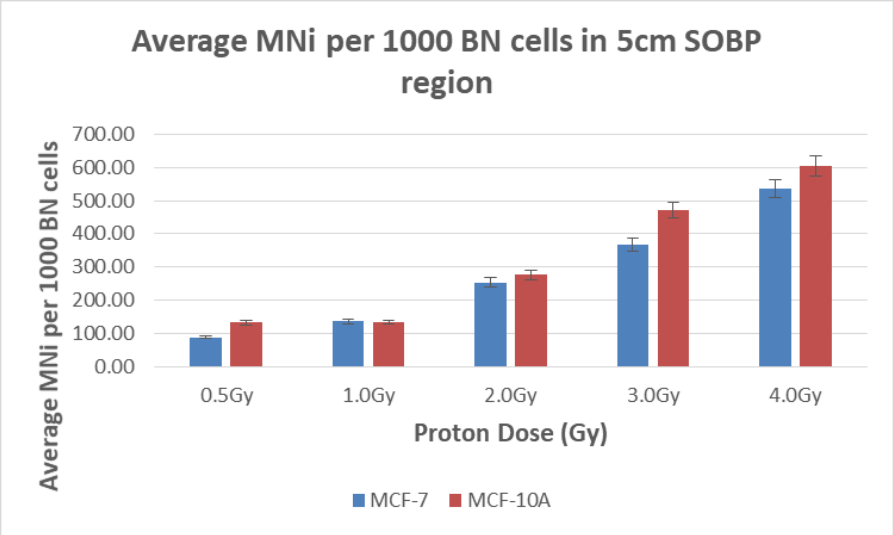

Figure 4.5: Average MNi scored per 1000 BN cells in the 5cm spread out Bragg peak for both breast cell lines.

Figure 4.4 – B, C &D show the MNi scored in the SOBP plateau (the 3 points: proximal, middle and distal parts of the SOBP also seen in Figure 4.5 as the average MNi in the SOBP region). Except for the 1 Gy (where both cell lines had 135 MNi per 1000 BN cells) the normal breast cells presented an increase sensitivity compared to the cancerous cell line in the 5 cm SOBP region.

Figure 4.4 - E represents MNi scored at the distal 80% on the depth dose curve (position 5) calibrated in water for both cell lines for each proton dose given. The radiosensitivity at the distal 80% region appears similar for both cell lines except for the higher dose of 4Gy where the normal cell line appears to be more radioresistant compared to the cancer cell line ($p < 0.0001$). However, this is not applicable to the other doses, so the 4 Gy sample of the MCF-10A cells might have received a too low dose (due to changes in the beam energy during the irradiation).

At the 40% depth at the distal end of the beam (Figure. 4.4 - F), the cancerous breast cell line showed an increased radioresistance compared with the normal breast cell lines for all dose points ($p < 0.001$).

Evaluating each position of the beam the evidence of this study indicated a difference in sensitivity between the two breast cell lines. The normal cell line were more sensitive, in general, compared to the cancerous breast cell line.

Figures 4.6 and 4.7 shows the MNi data and the fitted Linear Quadratic (LQ) curves using a non-linear regression analysis. In some cases, the β-values were negative after the initial fit. Since a negative β-value is indefinable, some data sets were refitted with a linear curve (β-value = 0).

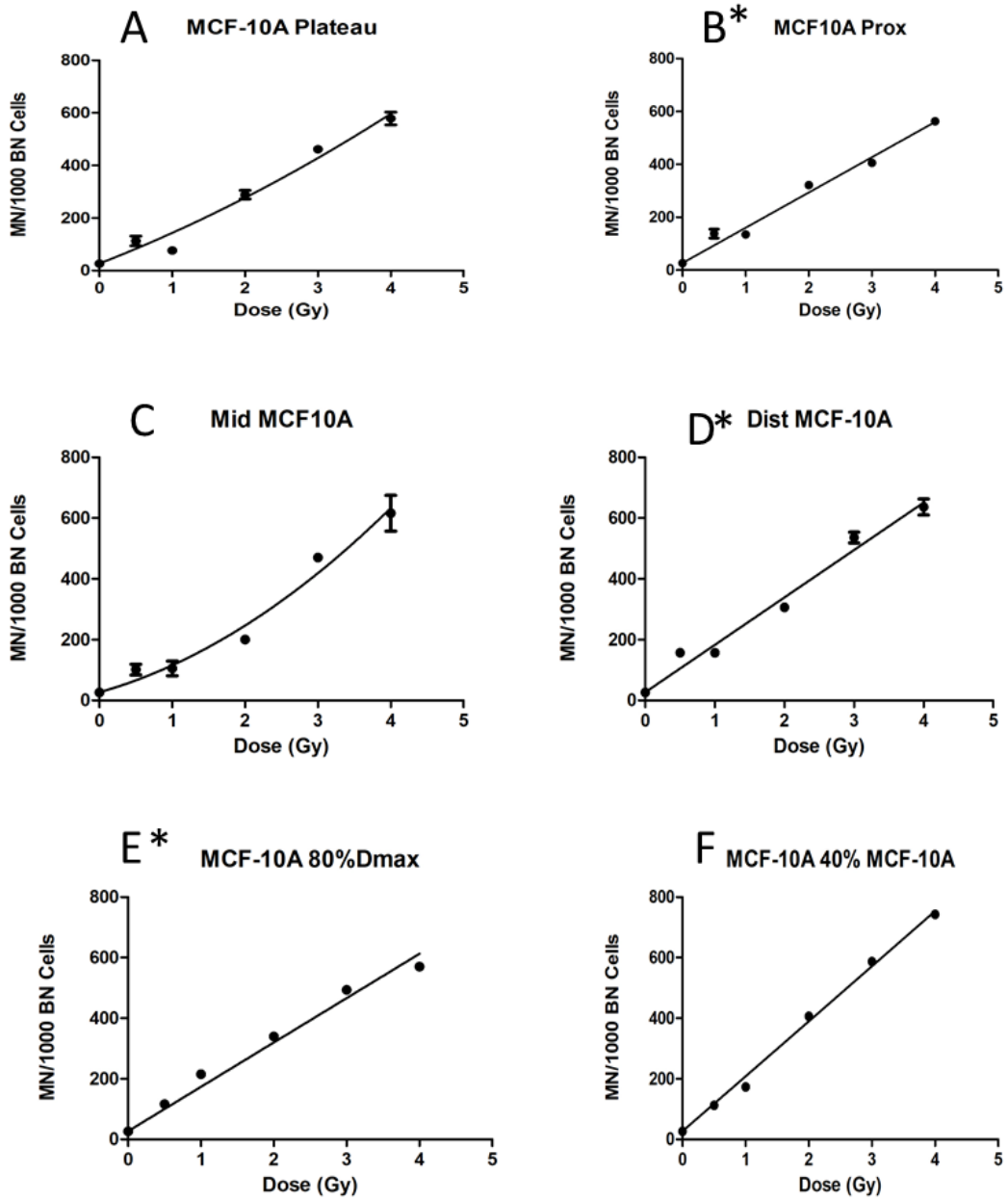

Figure 4.6: Best fit data graphs calculated from the MN formations per 1000 BN cells for the MCF-10A cells.

Best fits for all the MCF-10A cell lines MN data throughout the proton beam from the entrance plateau region (A) to the distal 40% region (F).(* graphs that were re-fitted).

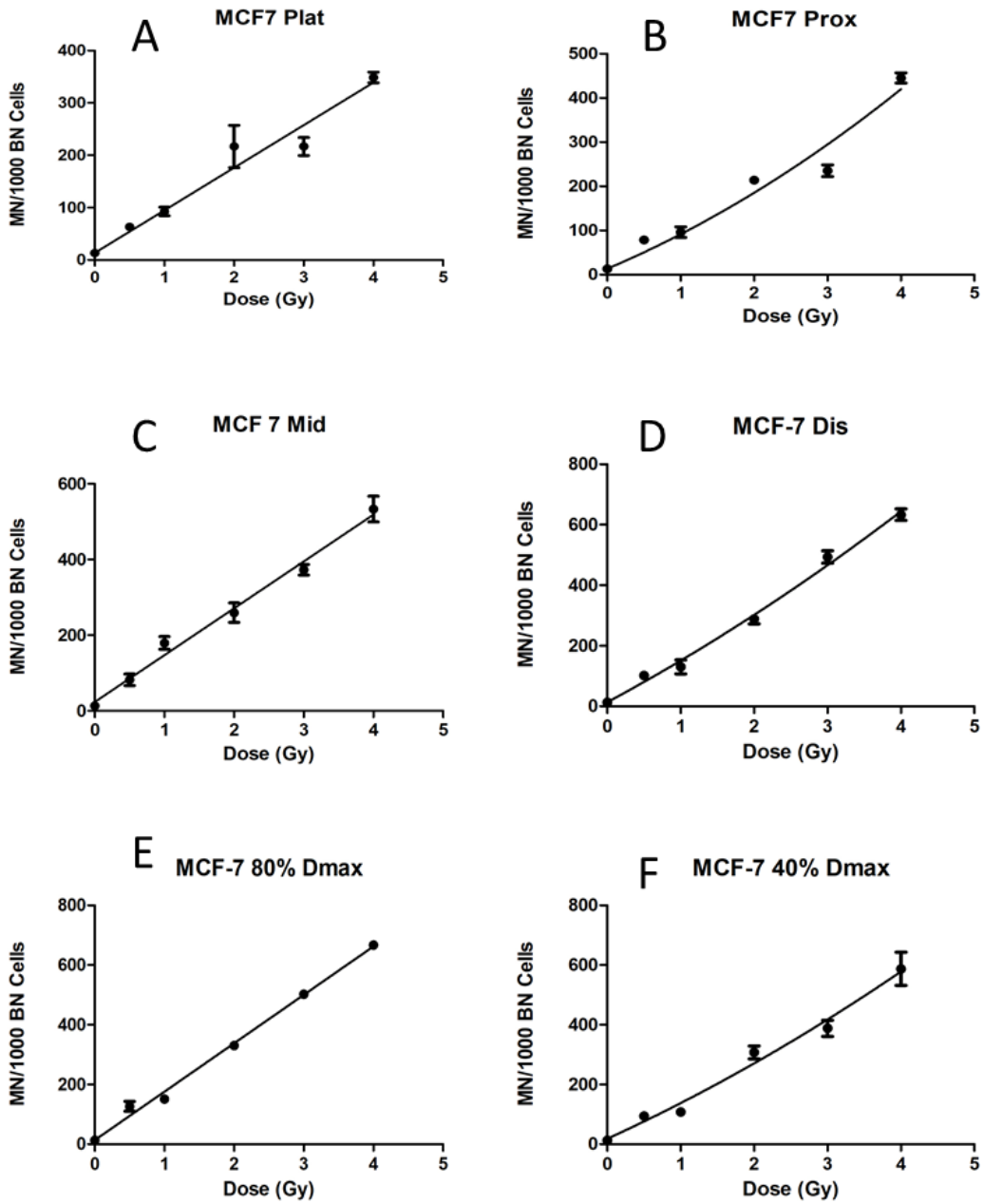

Figure 4.7: Best fit data graphs calculated from the MN formations per 1000 BN cells for the MCF-10A cells.
Best fits for all the MCF-10A cell lines MN data throughout the proton beam from the entrance plateau region (A) to the distal 40% region (F).

There was also a clear trend for increased MN with depth in sensitivity for both cell lines throughout the proton beam sections as indicated in Figure 4.8. Dose points of 2 Gy and 4 Gy chosen to demonstrate this tendency to use doses between 1.8 Gy and 4.0 Gy when treating breast cancer (Kacprowska and Jassem, 2012; Evans *et al.*, 2016; Yarnold, 2018). The linear sensitivity tendency increased from the reference region (plateau region) to the 40% depth for both the cancerous breast cell and the normal breast cell line (both $p < 0.0001$).

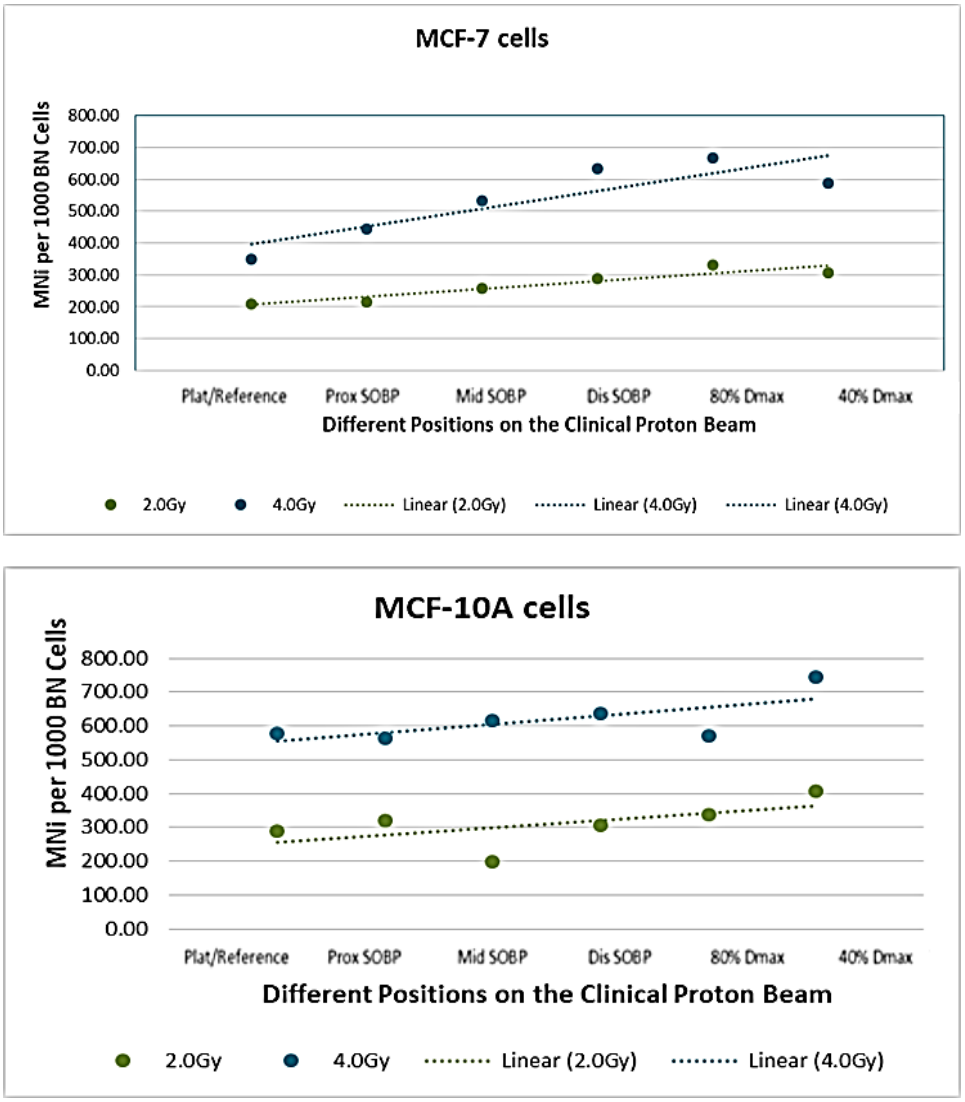

Figure 4.8: Trend lines for both breast cell lines throughout the proton beam. Both breast cell lines showing an increase in trend for MN formations per 1000 BN cell throughout the proton beam after 2 Gy and 4 Gy doses.

Table 2 indicates the coefficients of the fitted curves with coefficients of quadratic regression model for dose-response curves of micronucleus induction in both cell lines after exposure to protons at different positions.

Table 2: Alpha and beta values calculated in Graph Pad Prism using the second order polynomial theorem.

	Plateau region	Proximal SOBP region	Middle SOBP region	Distal SOBP region	Distal 80% region	Distal 40% region
Polynomial: Second Order (Y= A + B*X + C*X^2) Best-fit Values (MCF-10A)						
A (Background = a)	= 26.67	= 26.67	= 26.67	= 26.67	= 26.67	= 26.67
B (Bending component = α	113.10	140.70	67.96	157.20	192.60	181.10
C (Initial slope = β	7.25	-2.21	20.91	-0.32	-13.92	0.18
Polynomial: Second Order (Y= A + B*X + C*X^2) Best-fit values (MCF-7)						
A (Background = a)	= 13.33	= 13.33	= 13.33	= 13.33	= 13.33	= 13.33
B (Bending component = α	85.36	70.28	130.70	130.80	156.50	117.30
C (Initial slope = β	-1.34	7.84	-1.02	6.73	1.75	5.93

By solving the equation using the fitting parameters α and β in the using the quadratic formula (Equation 3), the dose in Gy could be calculated for different levels of biological effect (iso-effect). The RBE values could be calculated by the ratio of the dose at the different positions to the dose at the entrance plateau position for the same iso-effect starting from 100MN to 500MN for each cell line.

4.2 95% Confidence Ellipse Results

The ellipse region around a coordinate (the average MN frequency) for both MCF-7 and MCF-10A cells at the plateau region defined by the mean estimate of the α-value plotted on the X-axis and the β-value on the Y-axis is shown in Figure 4.9.

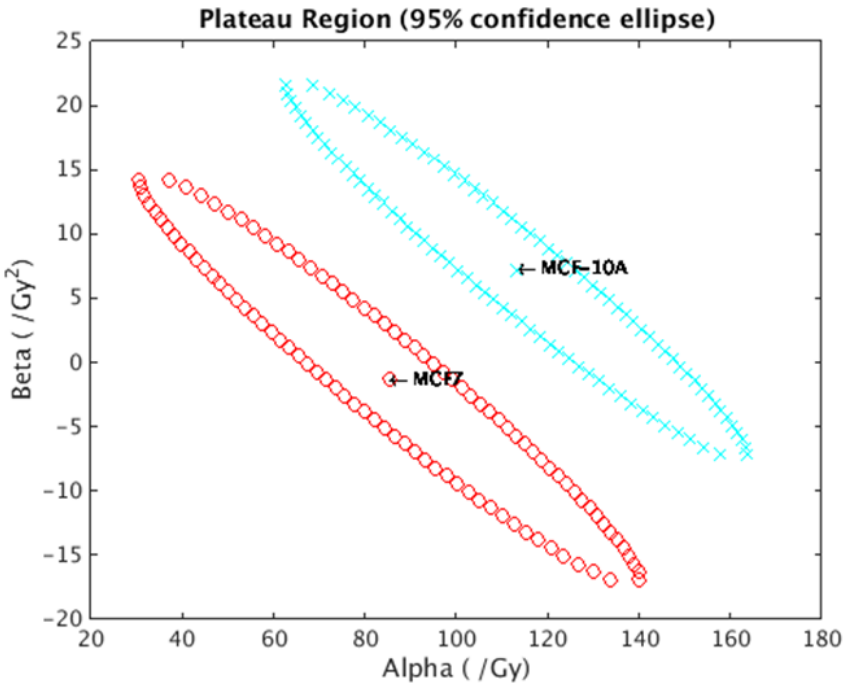

Figure 4.9: 95% confidence ellipses for both cell lines in the plateau region.
MCF-10A cells (turquoise) with a higher α/β ratio compared to the MCF-7 cells (red). Both ellipses are separated from each other.

The two ellipses do not overlap and therefore indicates an exclusive dose response relationship at the plateau in the proton beam. Meaning that, there is a significant difference in radiosensitivity between the MCF-7 and MCF-10A cell line.

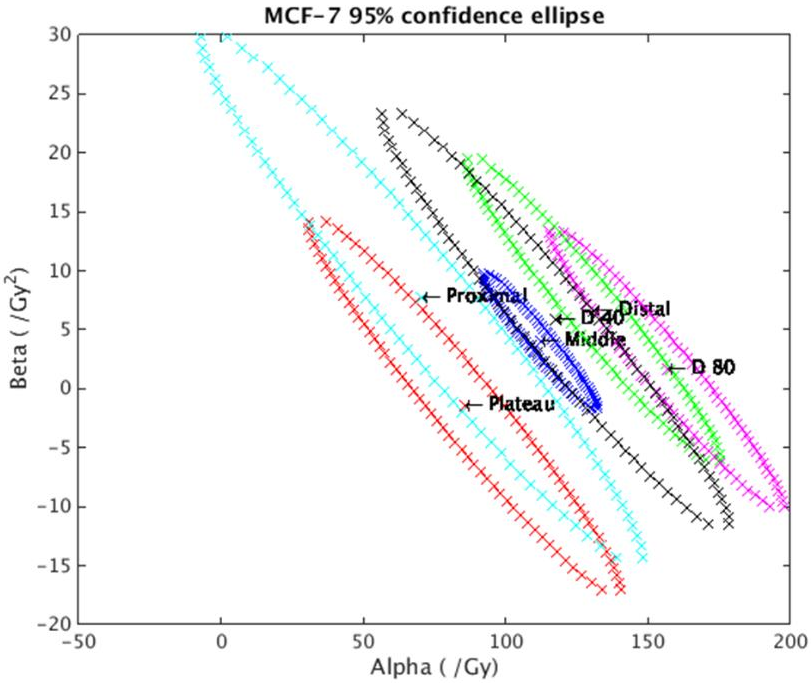

Figure 4.10: 95% Confidence ellipses for the MCF-7 cells for different regions in the proton beam.
Different ellipses were calculated. Some ellipses are clearly separated and others not for the MCF-7 cell lines.

The same method was then used to plot both the MCF-7 and MCF-10A cells as illustrated in Figures 4.10 and 4.11 respectively.

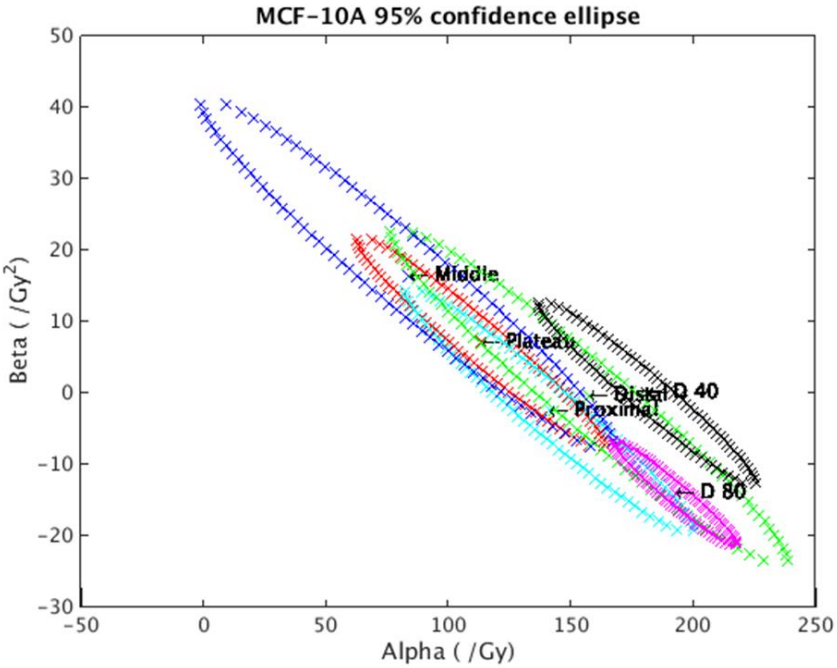

Figure 4.11: 95% Confidence ellipses for the MCF-10A cells for different regions in the proton beam.
Different ellipses were calculated and show that some ellipses are separated and others not for the MCF-7 cell lines. Most of these ellipses are much more compact compared to the MCF-10 cells.

The 95% confidence ellipse for MCF-7 cells do show overlap for the different positions. The entrance plateau region overlaps with the proximal SOBP region, but is clearly separated from the other regions. This indicates an exclusive dose response relationship for these positions compared to the other regions, and an increase in DNA damage with depth for the cancerous cell line. For the normal breast cells, the 95% ellipses indicate only a clear distinction between the D80% and D40% position from the reference (entrance plateau) position. When comparing the 95% confidence ellipses for the D40% of both cells, there is clear difference in the dose response relationship (Figure 4.12). This is in agreement with the observations obtained with the reference radiation, were isolated ellipses were also observed (Figure 4.10 and Figure 4.11).

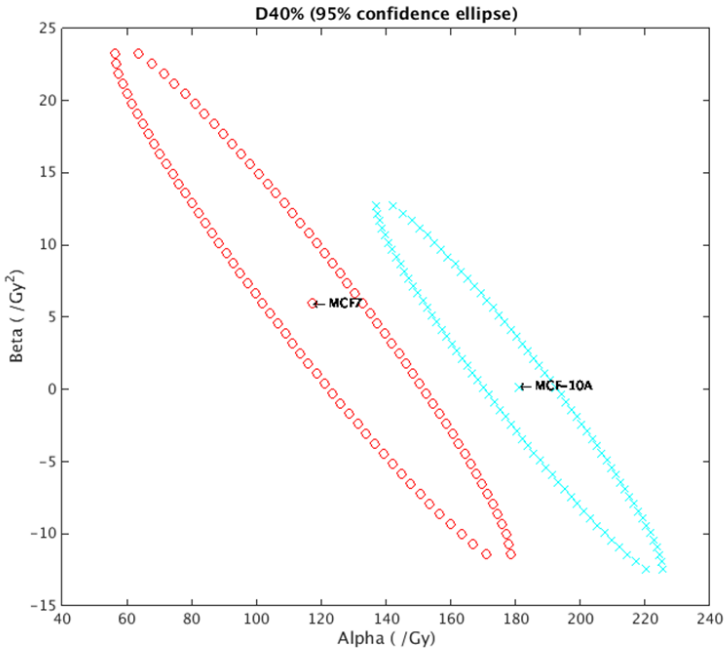

Figure 4.12: The 95% Confidence ellipses at the distal 40% for both cell lines. The 95% Confidence ellipse for the MCF-10 cell (turquoise) are shifted much more to the right of the graph indicating a higher α-value compared to the MCF-7 cells (red).

4.3 Variation in Relative Biological Effectiveness (RBE)

In order to calculate the RBE, the iso-effective doses were calculated for different levels of biological effect. Using equation 1 and Table 2 results, the iso-effective doses were calculated and for different MN frequencies, ranging from 100 up to 500 MNi/1000 BNCs. Table 3 and 4 demonstrate the iso-effective doses calculated for MCF10-A and MCF-7 cells respectively.

Table 3: Iso-effective doses calculated for the MCF-10A cells at different levels of biological effects.

Normalised to MNi	Dose (Gy) for MCF-10A					
	Plat/Reference	Prox SOBP	Mid SOBP	Dis SOBP	80% Dmax	40% Dmax
100	0.65	0.55	0.85	0.47	0.50	0.41
200	1.44	1.30	1.68	1.11	1.18	0.96
300	2.16	2.05	2.34	1.75	1.87	1.51
400	2.82	2.80	2.90	2.39	2.55	2.06
500	3.44	3.55	3.4	3.03	3.23	2.61

Table 4: Iso-effective doses calculated for the MCF-7 cells at different effects.

Normalised to MNi	Dose (Gy) for MCF-7					
	Plat/Reference	Prox SOBP	Mid SOBP	Dis SOBP	80% Dmax	40% Dmax
100	1.06	1.10	0.67	0.64	0.55	0.71
200	2.26	2.14	1.45	1.34	1.18	1.48
300	3.55	3.04	2.23	1.99	1.80	2.20
400	4.90	3.84	3.03	2.61	2.41	2.88
500	6.33	4.58	3.84	3.20	3.01	3.52

For the normal cells, the dose decrease throughout the proton beam from 1.44 Gy to 0.96 Gy for 200 MNi/1000 BNCs and from 2.82 Gy to 2.06 Gy for 400 MNi/1000 BNCs as indicated in Table 3. The MCF-7 cells indicate that when a similar radiobiological effect of 200 MNi/1000 BNCs, the proton dose decreases from 2.26 Gy in the entrance plateau to 1.48 Gy at 40% Dmax. For an effect of 400 MNi/1000 BNCs the dose decreased from 4.90 Gy to 2.88 Gy for the cancerous breast cell lines (Table 4).

Thereafter, the RBE values were calculated for each position based on the ratio of the iso-effective doses. The beam at the position of the entrance plateauwas used as the reference radiation in this study. The RBE was calculated for the MCF-10A cell line at different levels of biological effect as seen in Figure 4.13. With the increase in dose (also radiobiological effect) it is clear that the RBE decrease for the MCF-10A cells. Furthermore, it was observed that there was a sharp increase of RBE with depth throughout the proton beam, from a minimum of 1.05 to a maximum of 1.43 for an iso-effect of 300 MN/1000 BNCs.

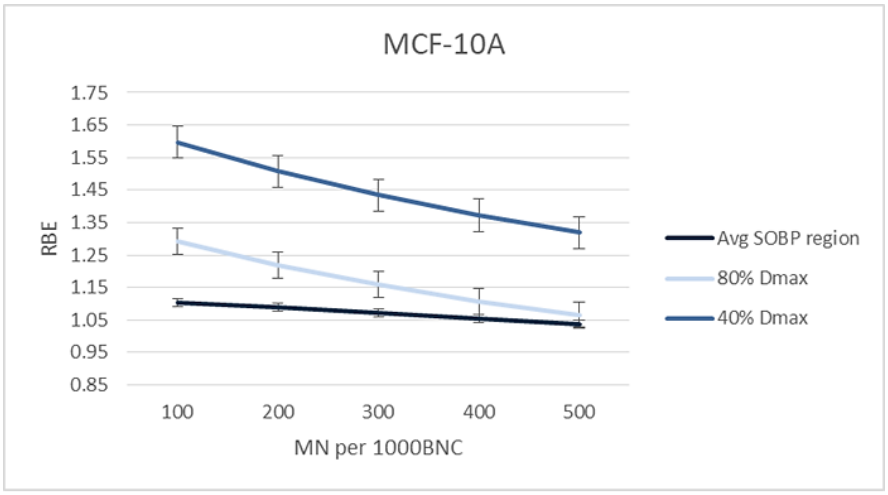

	RBE calculated for MCF-10A cells				
Normilized to Mni	Prox SOBP	Mid SOBP	Dis SOBP	80% Dmax	40% Dmax
100	1.18	0.76	1.38	1.29	1.60
200	1.11	0.86	1.30	1.22	1.51
300	1.05	0.92	1.24	1.16	1.43
400	1.01	0.97	1.18	1.11	1.37
500	0.97	1.01	1.14	1.06	1.32
Normilized to Mni	Avg SOBP region			80% Dmax	40% Dmax
100	1.10			1.29	1.60
200	1.09			1.22	1.51
300	1.07			1.16	1.43
400	1.05			1.11	1.37
500	1.04			1.06	1.32

Figure 4.13: RBE calculated based on the plateau region as reference radiation for the MCF-10A cells.

The RBE calculated for the MCF-7 cell line can be seen in Figure 4.14. However, in this case, the RBE increases with iso-effective dose or biological effect. For the cancer cells, there is also a sharp increase in RBE from 1.17 to 1.61 for an iso-effect of 300 MNi/1000 BNCs.

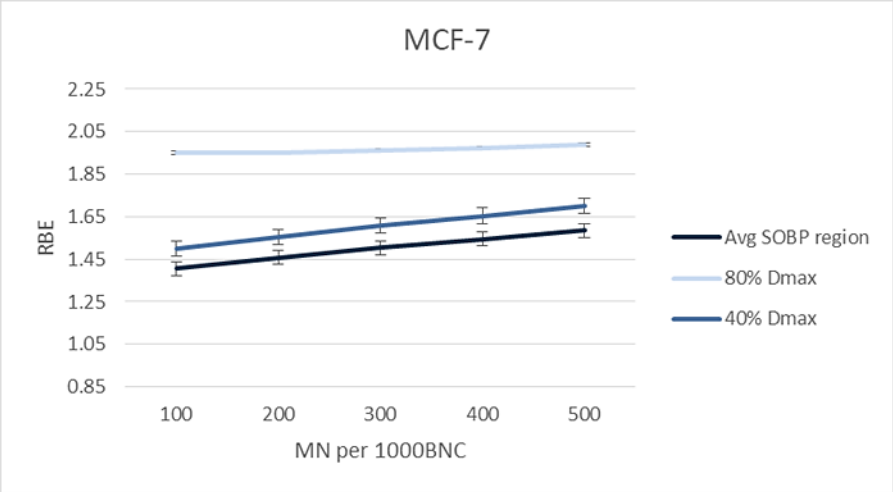

RBE calculated for MCF-7 cells					
Normilized to Mni	Prox SOBP	Mid SOBP	Dis SOBP	80% Dmax	40% Dmax
100	0.99	1.56	1.66	1.95	1.50
200	1.08	1.56	1.73	1.95	1.56
300	1.17	1.56	1.78	1.96	1.61
400	1.24	1.56	1.83	1.97	1.65
500	1.31	1.56	1.88	1.99	1.70
Normilized to Mni	Avg SOBP region			80% Dmax	40% Dmax
100	1.40			1.950	1.498
200	1.46			1.950	1.555
300	1.50			1.960	1.609
400	1.54			1.973	1.655
500	1.58			1.988	1.702

Figure 4.14: RBE calculated based on the plateau region as reference radiation for the MCF-7 cells.

After calculating the Pearson correlation to correlate RBE with position of the beam as shown in Table 5 between the two cells, the MCF-10A cell line showed a strong negative correlation at all positions in the beam, except at the mid SOBP region, implying that as the dose increase the RBE decreases. While the MCF-7 cell line showed a positive correlation for all positions, implying that for the cancerous cells as the dose increases the RBE also increases, this however was not expected.

Table 5: Pearson correlation coefficients for both cell lines.

	Prox SOBP	**Mid SOBP**	**Dis SOBP**	**80% Dmax**	**40% Dmax**
MCF-7	0.99983	0.99477	0.99930	0.99703	0.99999
MCF-10A	-0.99124	0.98285	-0.99340	-0.99709	-0.99273

In general the RBE increased with depth throughout the proton beam for both the cancerous and normal breast cell lines. For the cancerous cell lines the RBE increase significantly at the D80% region in the distal end of the proton beam however was found to be insignificant (p= 0.8968).

4.4 Bromodeoxyuridine (BrdU) and flow cytometric results

Assessing the S-phase fraction for each cell after BrdU and flow cytometric analysis reflected that the MCF-7 cells spend a longer time in the S-phase compared to the MCF-10A cells as seen in Figure 4.15.

The higher S-phase fraction of MCF-7 cells might explain the difference in radiosensitivity with the MCF-10A cells. Since the S-phase is the most radioresistant phase of the cell cycle, this could be an explanation why MCF-7 cells are more radioresistant than MCF-10A cells.

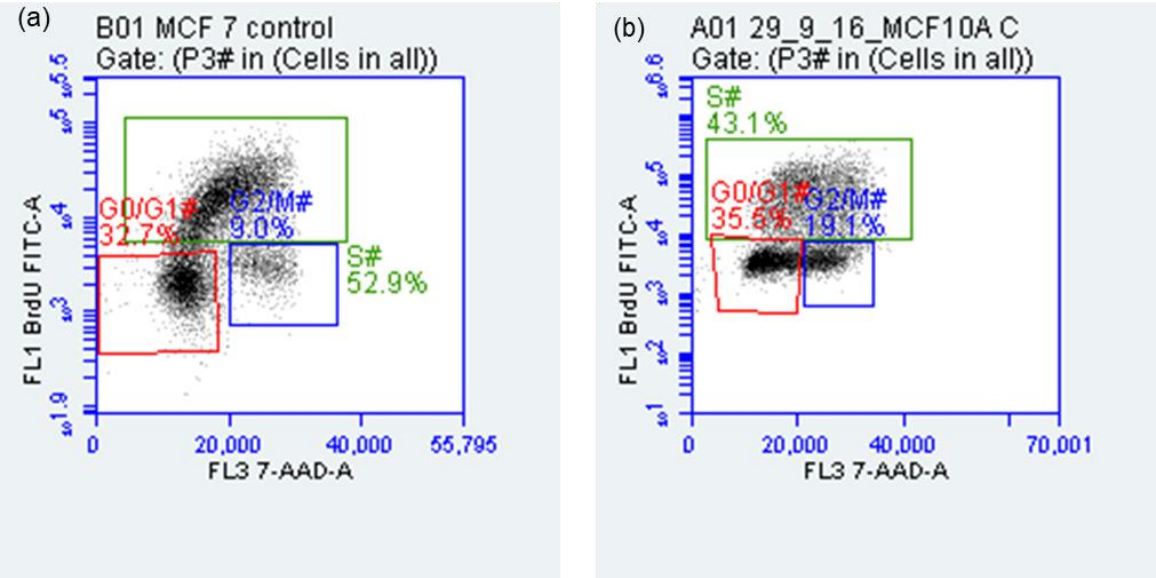

Figure 4.15: MCF-7 (a) and MCF-10A (b) cell-associated BrdU measured by flow cytometry

The MCF-7 cells spend 52.9% of time in the S-phase while MCF-10A spend almost 10% less time during the S-phase at 43.1%.

CHAPTER 5: DISCUSSION

***Overview**: The preliminary hypothesis as described in chapter 1 will in turn be compared to published literature. Furthermore, this chapter will highlight the clinical relevance and shortcomings combined with future perspectives.*

5.1 Background Readings

An important consideration to take into account in the MN assay is the background MN frequency (Hayashi, 2016). These were 13.33 ± 4.16 per 1000 BN for the MCF-7 cells and 26.67 ± 8.08 per 1000 BN for the MCF-10A cells. The background in MN frequency limits the sensitivity detection of damage induced by low doses of radiation (Mill et al., 1996). Our results are in agreement with previous studies, reporting background MN values ranging from 10 to 50 per 1000 BN cells for MCF-7 cells (Hewitt *et al.*, 2007; Shao *et al.*, 2008) and between 8.5 – 20 per 1000 BN cells for MCF-10A cells (Ottoboni *et al.*, 2001; Jdey *et al.*, 2017). In this study, the background MN frequency was subtracted from actual irradiated results for the data interpretation on both cell lines. In this way, the difference in background DNA damage did not influence the analysis and outcome of the results.

5.2 Variation in radiation sensitivity between the two breast cell lines

The main objective of this study was to understand the biological effect and response of protons on two different breast cell lines. It is well known that different breast cell lines respond differently to the same type of radiation treatment. In a study where Cobalt-60 radiation was used to investigate radiosensitivity of cell lines with both Clonogenic cell survival and DNA double strand break assays, it was clear that MCF10A cells were more radiosensitive compared to the cancerous cell lines (Villalobos et al., 1996). Radiosensitivity refers to the response to radiation (damage caused) and radioresponsiveness (including how cells modulate damage before final outcome) and differs between different tissue types (Hall and Cox, 2010). Several methods exists to measure cell radiosensitivity, e.g. one can measure the fraction of cells surviving a particular radiation dose (Begg, 2010), or fragments broken off from the chromosome after radiation (Scott et al., 1999; Rothfuss et al., 2000). This study evaluated the difference in radiosensitivity based on the entrance plateau position of the clinical proton beam as the reference radiation.

To the best of our knowledge, this is the first study where the MN assay was used to assess the genotoxic damage of a proton beam inflicted on the two breast cell lines. This method was previously used to explore radiosensitivity in Chinese hamster cells for low-energy protons (0.88 and 5.04 MeV), (Sgura et al., 2000).

The lowest dose used in this study was 0.5Gy and MN per 1000 BN cells did increase when compared to the controlled groups for both cells, indicating a significant increase was detectable associated to the background for DNA damage (Vral, Fenech and Thierens, 2011). A steady increase in MN formations was observed for both cell lines from the plateau region to the distal 80 percent, with a slight unexpected decrease in MN frequency at the distal 40% for the cancerous cell line could signifying that it may be relative to the preceding position after the SOBP as shown in Figure 5.1. Generally the cancerous cells were more radioresistant compared to the normal breast cell lines.

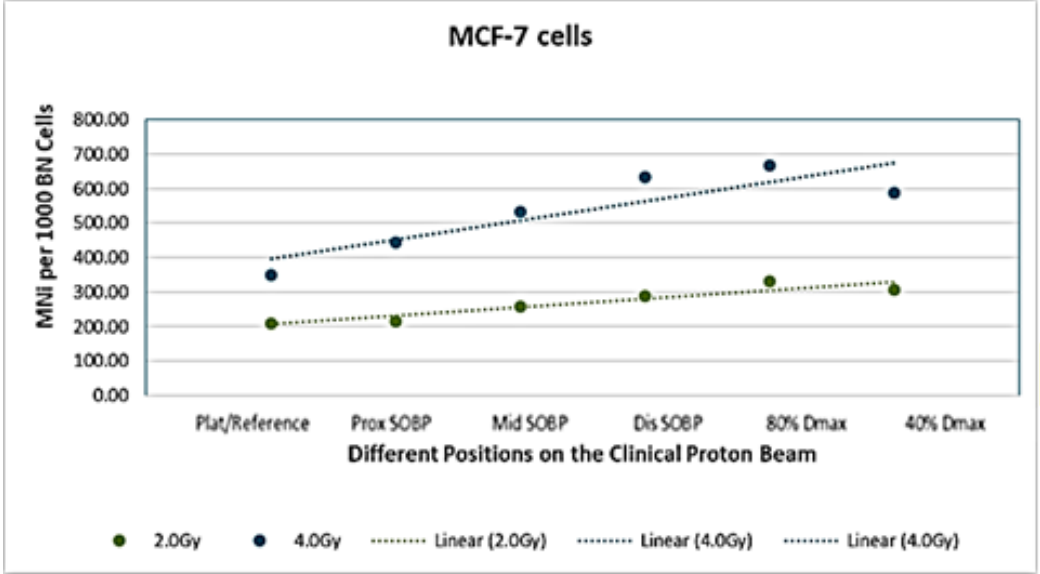

Figure 5.1: Difference in MN frequency for the cancerous cell lines (linear fit) at different depths along the SOBP for regularly used radiation doses (2Gy and 4Gy) for breast cancer patients.

The increase in biological damage per unit dose at the different depths is reflected in the RBE variation along the SOBP and in curves showing increased MN with dose e.g. Figures 4.6, 4.7. In this study the variation in RBE was between 0.99 to 1.99 and 0.92 to 1.6 for the cancerous cells (Figure 4.14) and the normal breast cell (Figure 4.13) respectively. Previous studies measured with the colony survival as biological end point reported RBE increases in the middle of the SOBP to 1.2 (Paganetti, 2003) and also from 1.1 to 1.23 at the middle of the SOBP when the SOBP was increased to 7cm also using a 200 MeV proton beam directed to intestinal crypt cells in mice (Gueulette et al., 1997). The distal edge region showed an increase in radiosensitivity for both cells which was in line with studies done for various cell lines using 2 Gy fractions, where RBE increases up to 1.35 on average at the distal fall-off were reported (Paganetti, 2014b). However, the distal 40% Dmax position did not coincide with previous studies, where a continuous increase in RBE in the far distal edge of the proton beam was reported (Paganetti, 2014a). This can possibly be explained by a variation in proton beam energy or beam characteristics during the experiment, resulting in a range uncertainty and output corrections were applied. The deviations in beam characteristics has been described by Zhao et al when output corrections are applied (Zhao et al., 2011).

5.2.1 95% Confidence Ellipse and Clinical Relevance

The confidence ellipses (shown in Figure 4.9) for the dose-response parameters for the two cell lines does not overlap for irradiations in the plateau region. This indicate a significant change in the radiation sensitivity of these two cell types to protons in this region of the Bragg curve. The β-value for the MCF-7 cells is not significantly different from zero indicating that whilst that for MCF-10A cells is significant. The clinical importance of this should be understood in terms of alpha/ beta ratios for protons for these two cell types. The zero β-value for MCF-7 cells may well be the result of the 3 Gy dose point that was somehow underestimated in the experimental work – Figure 4.9 (A). In order to compare alpha/beta ratio the β-value for the MCF-10A were used to fit the data for the MCF-7 cells. The alpha/beta ratio for MCF-7 cells is then calculated to be 8 Gy compare to 16 Gy for MCF10A cells.

The ratio of the two parameters, α/β, is a measure of the importance of fractionation in determining the biological effective dose (Ray, Sibson and Kiltie, 2015; Hawkins, 2017). From the data obtained and assumptions used, fractionated proton therapy the MCF10A cells will be repair less between fractions compared to the MCF7 cells. Thus the normal cells repair less to the cancer cells and is

stressed in a similar study comparing repair mechanisms between cancerous and normal cells (van Leeuwen *et al.*, 2018). If the responses of these cell lines are indicative of normal and tumour tissue responses in fractionated radiotherapy, it would suggest that there may not be therapeutic gain from extensive fractionation. However, for this reason, hypofractionated stereotactic treatment protocols that can be applied with protons may be to the befit of the patient (Laine *et al.*, 2015).

The above argument is based only on the radiosensitivity of the two cell lines when exposed in the plateau region. Further analysis of the 95% confidence ellipse of both cell lines also shows a clear increase of the alpha value toward the distal portion of the beam and suggests a possible increase in LET in this region. Considering that the α and β parameters gradually increase with depth for protons for both cell lines (Figure 24), of clinical importance is a non-homogeneous dose within the targeted area and an unwanted high dose behind the targeted area as emphasised in former studies for paediatric tumours (Jin et al., 2011; Jones et al., 2012) and distal energy modulation could be investigated especially with larger tumours (Buchsbaum *et al.*, 2014). It may be prudent that the modulation of the SOBP should be such that less radiation be applied to the distal part to keep the biological effectiveness the same (Flejmer *et al.*, 2015). A continued observation in view of the 95% confidence ellipses for the normal breast cells being much more compacted compared to the cancerous cells may indicate an increase in variance of radiosensitivity in the MCF-7 cells, based on the α-value, to proton radiation.

5.2.2 S-phase

Radiosensitivity also varies throughout the cell cycle with, in general, late S-phase being most radioresistant, G2/M being most radiosensitive and G1 phase taking an intermediate position (Hall, 1985; Gravina et al., 2010). Furthermore, cells that divide frequently are more radiation-sensitive than those that divide rarely (Yashar, 2012) thus, tissues that consist of rapidly dividing cells are similarly radiation-sensitive (Hafer, Rivina and Schiestl, 2010). The S-phase of the cell cycle occurs during interphase, in between the Gap phases, with the most important event being DNA replication. MCF-7 cells spend approximately 10% more time in the S-phase when compared to MCF-10A, this could possibly explain the increase in resistance of the MCF-7 cells. However, a small percentage variation could be discounted as the error bars are considered as the graphical representation of the variability of this data and indicate the uncertainty of this measurement. Nevertheless, DNA synthesis for cancer cell lines are extended as doubling time for MCF-7 cells is 34 hours, while MCF-10A has a doubling time of 16 hours (Gueulette et al., 1997; Coller, 2007; Cecchini, Amiri and Dick, 2012; Corbin et al., 2017). MCF-10A cells are known to grow faster, therefore the result that MCF-7 cells are more resistant than MCF-10A is intriguing. Based on the BrdU assay and flow cytometry results, a possible explanation could be the variation during the doubling time in each culture although the overall doubling time (of these two cell lines) is not the best way to infer length of S-phase.

A comparison of these two cell lines on the BrdU results which found that the MCF-10 cell were more sensitive than the MCF-7 cells. It is important to note here, that this is not based on their doubling time as expressed by other similar investigations (Theron *et al.*, 1997; Pajonk, Vlashi and McBride, 2010).

5.3 Variation in the Relative Biological Effectiveness (RBE) in Relation to Dose

The dose given to a breast cancer patient when using protons are usually the photon-equivalent dose divided by the RBE. If the RBE allocations differ it can result in an under- or overdose to both the target and the normal tissue as only a single RBE is used. This could have legal implications based on a 2% dose precision regulation (Dale, Jones and Carabe-Fernandez, 2009; Anferov and Das, 2015). However, these guidelines does not incorporate RBE into the standard operating procedures but only refer to physical dose. With a considerable iso-effective dose variations (Tables 3 and 4), the RBE results (Figures 4.15 and 4.16) for the normal breast cells undergoing proton irradiation are supported by previous studies. (Levin *et al.*, 2005; Mcnamara *et al.*, 2012; Girdhani, Sachs and Hlatky, 2013; Lühr *et al.*, 2018), As a basic rule, the RBE increases with decreasing dose and is occasionally

higher for late effects than for early effects, especially at low doses (McNamara, Schuemann and Paganetti, 2015). The significant RBE increase in depth for both cell lines can possibly be explained by the linear trend to increase of the α-value (Figure 5.2) and therefore was consistent with literature that it can indicate an increase in LET (Britten *et al.*, 2013; Villagrasa *et al.*, 2014).

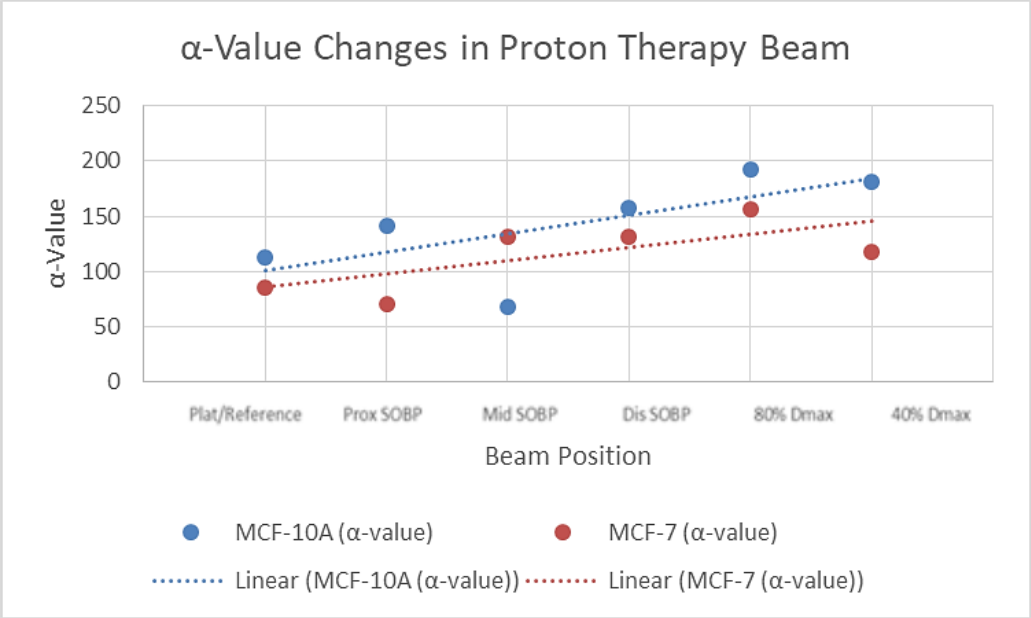

Figure 5.2: Difference in α-value and tendency (linear fit) for the two cell lines at different positions of the proton beam.

The increase in RBE with the increase in dose for the cancerous cells could be attributed to the β-value being close to zero in the plateau region which was used as reference to calculate the RBE. It is also possible that due the large α component in the plateau region, the value of β becomes negligible, indicative of no exponential component in this region, which suggests the existence of a small anti-correlation between the Linear Quadratic (LQ) parameters. Unlike the α component, the β-value does not change as prominent when the radiation shifts from low LET to high LET and therefore less of an indication of an increases in LET but rather the small change in response per unit dose (Moignier *et al.*, 2014). Furthermore, the proton RBE calculated in this study used proton beam in the entrance plateau as the reference radiation, and these results therefore only indicates the variation within the clinical proton beam.

5.4 Recommendations and Limitations

Owing to the assumption of an increase in the LET at the distal part of the proton beam, the possibility of erroneous radiation treatment could be minimised with beam modulation as found in this study. Moreover, the increased repair capability of the cancerous breast cells compared to normal breast cells when fractionated proton radiation therapy are to be applied is indicated by the α/β ratio of the survival curve. The need of hypofractionation should therefore be considered.

This study, however, is not in agreement with previous reported results where the RBE for protons decreased with an increase in dose for the cancerous breast cells (Takatsuji, Yoshikawa and Sasaki, 1999; Friedrich et al., 2013; Paganetti, 2014b). Therefore, to verify these findings a replication of this study must be considered. The variation in radiation sensitivity, especially observed with the cancerous cells, could also be attributed to the proton beam quality and real time dose monitoring should be considered in similar future studies. Conventional radiation treatment planning methods should be reassessed and a more adaptive method such as LET-painting could potentially give an enhanced tumour effect compared to conventional particle therapy (Malinen and Sovik, 2015). Since

the RBE increased for lower doses and the linear quadratic model in the lower dose region has been questioned during this study, it is beneficial for lower dose values to be incorporated in future studies. Although this study indicated a clear variation in radiosensitivity for the two breast cancer cell lines, future investigations should consider more radiobiological endpoints for example, DNA-damage repair, by using γ-H2AX localisation and therefore focus on repair-related factors (Redon *et al.*, 2009).

CHAPTER 6: CONCLUSIONS

Breast cancer is the most commonly diagnosed cancer among woman in South Africa (Herbst, 2015), almost half a million woman dying of this disease (Cancer Research UK, 2012). Therefore, a resilient purpose should be focused on treatment efforts. Although technological advances made in conventional radiotherapy to treat breast cancer, protons could have a favourable results compared to photons for example by decreasing cardiac morbidity (Xu et al., 2014). However, the concern around the uncertainties in RBE and LET at the distal region of the beam close to critical structures remains a major concern (Tommasino and Durante, 2015). This study suggests that hypofractionation and beam modulation could possibly improve the outcome for the treatment of breast cancer. Conventionally, the ability to deliver large doses of radiation to a tumour has been limited by radiation-induced toxicity to normal surrounding tissues.

However, advances in proton radiation delivery techniques and image guidance have allowed for more ablative doses of radiation to be delivered in a very accurate, conformal, and safe manner with shortened fractionation schemes. Additionally, hypofractionation is able to deliver a complete course of radiation therapy over a shorter period of time compared to conventional fractionation regimens making treatment more convenient to the patient and potentially more cost-effective. The improved target coverage and normal tissue avoidance over conventional photon techniques are well established. Proton therapy already became an attractive modality to further investigate the role of hypofractionation in the treatment of breast tumours. Applying hypofractionated regimens, the potential clinical advantage of proton therapy could be achieved when treating breast cancer.

The MN assay was used as a suitable biological endpoint for normal tissue complications, radiosensitivity and late effects. In this study, we explored the radiosensitivity differences for two cell lines, including a normal and a cancerous breast cell line, and observed significant increases in RBE along the depth dose profile of protons. While more biological endpoints and in vivo models could have improved the understanding of proton radiobiology, this study adds significant information to the existing evidence base that there is an increase in RBE in the distal fall-off region relative to the proton beam entrance plateau. The debate on variable versus constant proton RBE of 1.1 in PT treatment planning is still ongoing. Disregarding RBE variations could lead to suboptimal proton plans, resulting in lower doses to the tumour and hot spots in organs at risk. Although several studies have highlighted the importance and impact of variable RBE values with depth in proton treatment planning, it is currently not applied in clinical practice. Therefore, the results of this study could be used by the modelling community to further develop biologically motivated treatment planning for proton therapy.

CHAPTER 7:REFERENCES

Abolfath, R. *et al.* (2017) 'A model for relative biological effectiveness of therapeutic proton beams based on a global fit of cell survival data', *Scientific Reports*, 7(1), p. 8340. doi: 10.1038/s41598-017-08622-6.

Alexandru, D. and Iuliana, T. (2012) 'Impact of variable RBE on proton fractionation', *Medical Physics*. Wiley-Blackwell, 40(1), p. 11705. doi: 10.1118/1.4769417.

Ando, K. *et al.* (2001) 'Relative Biological Effectiveness of the 235 MeV Proton Beams at the National Cancer Center Hospital East', *Journal of Radiation Research*, 42(1), pp. 79–89.

Ando, K. and Kase, Y. (2009) 'Biological characteristics of carbon-ion therapy', *International Journal of Radiation Biology*, 85(9), pp. 715–728. doi: 10.1080/09553000903072470.

Anferov, V. and Das, I. J. (2015) 'Biological Dose Estimation Model for Proton Beam Therapy', *International Journal of Medical Physics, Clinical Engineering and Radiation Oncology*, 4(May), pp. 149–161. doi: http://dx.doi.org/10.4236/ijmpcero.2015.42019.

Antoccia, A. *et al.* (2009) 'Cell cycle perturbations and genotoxic effects in human primary fibroblasts induced by low-energy protons and X/gamma-rays.', *Journal of radiation research*. 50(5), pp. 457–468.

Ares, C. *et al.* (2010) 'Postoperative Proton Radiotherapy for Localized and Locoregional Breast Cancer: Potential for Clinically Relevant Improvements?', *International Journal of Radiation Oncology Biology Physics*., 76(3), pp. 685–697. doi: 10.1016/j.ijrobp.2009.02.062.

Arib, M., Medjadj, T. and Boudouma, Y. (2006) 'Study of the influence of phantom material and size on the calibration of ionization chambers in terms of absorbed dose to water', *Journal of Applied Clinical Medical Physics*, 7(3), pp. 55–64. doi: 10.1120/jacmp.v7i3.2264.

Baek, H.-J. *et al.* (2008) 'Radiobiological characterization of proton beam at the National Cancer Center in Korea.', *Journal of radiation research*. England, 49(5), pp. 509–515.

Barendsen, G. (1979) *Influence of Radiation Quality on the Effectiveness of Small Doses for Induction of Reproductive Death and Chromosome Aberrations in Mammalian Cells*, *International journal of radiation biology and related studies in physics, chemistry, and medicine*. doi: 10.1080/09553007914550811.

Barnett, G. C. *et al.* (2009) 'Normal tissue reactions to radiotherapy: towards tailoring treatment dose by genotype', *Nature Reviews Cancer*, 9, p. 134.

Begg, A. C. (2010) '5 - Prediction of Radiation Response A2 - Hoppe, Richard T.', in Phillips, T. L. and Roach, M. B. T.-L. and P. T. of R. O. (Third E. (eds). Philadelphia: Content Repository Only, pp. 69–81. doi: https://doi.org/10.1016/B978-1-4160-5897-7.00005-6.

Bentzen, S. M. (2006) 'Preventing or reducing late side effects of radiation therapy: radiobiology meets molecular pathology.', *Nature reviews. Cancer*, 6(9), pp. 702–713. doi: 10.1038/nrc1950.

Bradley, J. A. *et al.* (2016) 'Initial Report of a Prospective Dosimetric and Clinical Feasibility Trial Demonstrates the Potential of Protons to Increase the Therapeutic Ratio in Breast Cancer Compared With Photons.', *International journal of radiation oncology, biology, physics*, 95(1), pp. 411–421. doi: 10.1016/j.ijrobp.2015.09.018.

Bradshaw, P. T. *et al.* (2016) 'Cardiovascular Disease Mortality Among Breast Cancer Survivors', *Epidemiology,* 27(1), pp. 6–13. doi: 10.1097/EDE.0000000000000394.

Brenner, D. J. *et al.* (2009) 'Reduction of the secondary neutron dose in passively scattered proton radiotherapy, using an optimized pre-collimator/collimator', *Physics in medicine and biology*, 54(20), pp. 6065–6078. doi: 10.1088/0031-9155/54/20/003.

Brenner, D. J. *et al.* (2014) 'Risk and risk reduction of major coronary events associated with

contemporary breast radiotherapy.', *JAMA internal medicine*, 174(1), pp. 158–160. doi: 10.1001/jamainternmed.2013.11790.

Britten, R. A. *et al.* (2013) 'Variations in the RBE for cell killing along the depth-dose profile of a modulated proton therapy beam.', *Radiation research*. United States, 179(1), pp. 21–28. doi: 10.1667/RR2737.1.

Buchsbaum, J. C. *et al.* (2014) 'Range modulation in proton therapy planning: a simple method for mitigating effects of increased relative biological effectiveness at the end-of-range of clinical proton beams', *Radiation Oncology*. BioMed Central, 9, p. 2. doi: 10.1186/1748-717X-9-2.

Buwenge, M. *et al.* (2017) 'Intensity modulated radiation therapy for breast cancer: current perspectives', *Breast Cancer : Targets and Therapy*. Dove Medical Press, 9, pp. 121–126. doi: 10.2147/BCTT.S113025.

Calugaru, V. *et al.* (2011) 'Radiobiological characterization of two therapeutic proton beams with different initial energy spectra used at the Institut Curie Proton Therapy Center in Orsay.', *International journal of radiation oncology, biology, physics*. United States, 81(4), pp. 1136–1143. doi: 10.1016/j.ijrobp.2010.09.003.

Camarillo, I. G. *et al.* (2014) '4 - Low and high voltage electrochemotherapy for breast cancer: an in vitro model study BT - Electroporation-Based Therapies for Cancer', in. Woodhead Publishing, pp. 55–102. doi: https://doi.org/10.1533/9781908818294.55.

Carante, M. Pietro and Ballarini, F. (2016) 'Calculating Variations in Biological Effectiveness for a 62 MeV Proton Beam', *Frontiers in Oncology*, 6, p. 76. doi: 10.3389/fonc.2016.00076.

Chan, T. Y., Tan, P. W. and Tang, J. I. (2017) 'Intensity-modulated radiation therapy for early-stage breast cancer: is it ready for prime time?', *Breast Cancer : Targets and Therapy*. Dove Medical Press, 9, pp. 177–183. doi: 10.2147/BCTT.S127583.

Chang, E. *et al.* (2018) 'Association between prolonged metastatic free interval and recurrent metastatic breast cancer survival: findings from the SEER database.', *Breast cancer research and treatment*. doi: 10.1007/s10549-018-4968-7.

Chaudhary, P. *et al.* (2016) 'Variations in the Processing of DNA Double-Strand Breaks Along 60-MeV Therapeutic Proton Beams.', *International journal of radiation oncology, biology, physics*, 95(1), pp. 86–94. doi: 10.1016/j.ijrobp.2015.07.2279.

Cheng, Y. *et al.* (2017) 'Long-Term Cardiovascular Risk After Radiotherapy in Women With Breast Cancer'. doi: 10.1161/JAHA.117.005633.

Chuai, Y. *et al.* (2012) 'Molecular hydrogen and radiation protection.', *Free radical research,* 46(9), pp. 1061–1067. doi: 10.3109/10715762.2012.689429.

Clarke, M. *et al.* (2005) 'Effects of radiotherapy and of differences in the extent of surgery for early breast cancer on local recurrence and 15-year survival: an overview of the randomised trials', *Lancet*, 366. doi: 10.1016/S0140-6736(05)67887-7.

Corbin, K. S. and Mutter, R. W. (2018) 'Proton therapy for breast cancer : progress & pitfalls', 7.

Corradini, S., Niyazi, M., *et al.* (2018) 'Adjuvant radiotherapy after breast conserving surgery – A comparative effectiveness research study', *Radiotherapy and Oncology*, 114(1), pp. 28–34. doi: 10.1016/j.radonc.2014.08.027.

Corradini, S., Ballhausen, H., *et al.* (2018) 'Left-sided breast cancer and risks of secondary lung cancer and ischemic heart disease : Effects of modern radiotherapy techniques.', *Strahlentherapie und Onkologie : Organ der Deutschen Rontgengesellschaft ... [et al]*, 194(3), pp. 196–205. doi: 10.1007/s00066-017-1213-y.

Cuaron, J. J. *et al.* (2015) 'Early Toxicity in Patients Treated With Postoperative Proton Therapy for Locally Advanced Breast Cancer', *International journal of radiation oncology, biology, physics*, 92(2), pp. 284–291. doi: 10.1016/j.ijrobp.2015.01.005.

Cuaron, J. J., MacDonald, S. M. and Cahlon, O. (2016) 'Novel applications of proton therapy in breast carcinoma', *Chinese clinical oncology*, 5(4), p. 52. doi: 10.21037/cco.2016.06.04.

Dale, R. G., Jones, B. and Carabe-Fernandez, A. (2009) 'Why more needs to be known about RBE effects in modern radiotherapy.', *Applied radiation and isotopes : including data, instrumentation and methods for use in agriculture, industry and medicine*, 67(3), pp. 387–392. doi: 10.1016/j.apradiso.2008.06.013.

Darby, S. C. *et al.* (2005) 'Long-term mortality from heart disease and lung cancer after radiotherapy for early breast cancer: prospective cohort study of about 300,000 women in US SEER cancer registries.', *The Lancet. Oncology*., 6(8), pp. 557–565. doi: 10.1016/S1470-2045(05)70251-5.

Darby, S. C. *et al.* (2013) 'Risk of Ischemic Heart Disease in Women after Radiotherapy for Breast Cancer', *New England Journal of Medicine*, 368(11), pp. 987–998. doi: 10.1056/NEJMoa1209825.

Dawson, P. J. *et al.* (1996) 'MCF10AT: a model for the evolution of cancer from proliferative breast disease.', *The American Journal of Pathology*, 148(1), pp. 313–319.

Debnath, J., Muthuswamy, S. K. and Brugge, J. S. (2003) 'Morphogenesis and oncogenesis of MCF-10A mammary epithelial acini grown in three-dimensional basement membrane cultures', *Methods*, 30. doi: 10.1016/S1046-2023(03)00032-X.

Dennis, E. R. *et al.* (2013) 'A Comparison of Critical Structure Dose and Toxicity Risks in Patients with Low Grade Gliomas Treated with IMRT versus Proton Radiation Therapy', *Technology in Cancer Research & Treatment*. Elsevier Inc., 12(1), pp. 1–9. doi: 10.7785/tcrt.2012.500276.

Diener-West, M. *et al.* (2001) 'The COMS randomized trial of iodine 125 brachytherapy for choroidal melanoma, III: initial mortality findings. COMS Report No. 18.', *Archives of ophthalmology (Chicago, Ill. : 1960)*. United States, 119(7), pp. 969–982.

Early Breast Cancer Trialists Collaborative Group (EBCTCG)* (2005) 'Effects of radiotherapy and of differences in the extent of surgery for early breast cancer on local recurrence and 15-year survival: An overview of the randomised trials', *Lancet*, 366(9503), pp. 2087–2106. doi: 10.1016/S0140-6736(05)67887-7.

Elmekawy, A. *et al.* (2014) 'SU-E-J-49: Distal Edge Activity Fall Off Of Proton Therapy Beams', *Medical Physics*, 41(Part7), p. 166. doi: 10.1118/1.4888101.

Emami, B. (2013) 'Tolerance of Normal Tissue to Therapeutic Radiation', *Reports of Radiotherapy and Oncology*, 1(1), pp. 36–48. doi: 10.1016/0360-3016(91)90171-Y.

Evans, S. B. *et al.* (2016) 'Standardizing dose prescriptions: An ASTRO white paper', *Practical Radiation Oncology*. American Society for Radiation Oncology, 6(6), pp. e369–e381. doi: 10.1016/j.prro.2016.08.007.

Fenech, M. *et al.* (2003) 'HUMN project: detailed description of the scoring criteria for the cytokinesis-block micronucleus assay using isolated human lymphocyte cultures.', *Mutation research*, 534(1–2), pp. 65–75.

Fenech, M. (2007) 'Cytokinesis-block micronucleus cytome assay.', *Nature protocols*, 2(5), pp. 1084–1104. doi: 10.1038/nprot.2007.77.

Fisher, B. *et al.* (2002) 'Twenty-Year Follow-up of a Randomized Trial Comparing Total Mastectomy, Lumpectomy, and Lumpectomy plus Irradiation for the Treatment of Invasive Breast Cancer', *New England Journal of Medicine*, 347(16), pp. 1233–1241. doi: 10.1056/NEJMoa022152.

Flejmer, A. M. *et al.* (2015) 'Potential Benefit of Scanned Proton Beam versus Photons as Adjuvant Radiation Therapy in Breast Cancer', *International Journal of Particle Therapy*, 1(4), pp. 845–855. doi: 10.14338/IJPT-14-00013.1.

Fontenot, J. D., Newhauser, W. D. and Titt, U. (2005) 'Design tools for proton therapy nozzles based on the double-scattering foil technique.', *Radiation protection dosimetry*, 116(1–4 Pt 2), pp. 211–215.

Foote, R. L. *et al.* (2012) 'The clinical case for proton beam therapy.', *Radiation oncology (London,*

England), 7, p. 174. doi: 10.1186/1748-717X-7-174.

Frandsen, J. *et al.* (2015) 'Increased risk of death due to heart disease after radiotherapy for esophageal cancer', *Journal of Gastrointestinal Oncology*, 6(5), pp. 516–523. doi: 10.3978/j.issn.2078-6891.2015.040.

Friedland, W. *et al.* (2003) 'Simulation of DNA damage after proton irradiation.', *Radiation research*, 159(3), pp. 401–410.

Friedrich, T. *et al.* (2012) 'Calculation of the biological effects of ion beams based on the microscopic spatial damage distribution pattern.', *International journal of radiation biology*, 88(1–2), pp. 103–107. doi: 10.3109/09553002.2011.611213.

Friedrich, T. (2016) 'Biophysical modeling of effects of ionizing radiation and associated uncertainties'.

Fu, Q. *et al.* (2012) 'Response of cancer stem-like cells and non-stem cancer cells to proton and γ-ray irradiation', *Nuclear Instruments and Methods in Physics Research Section B: Beam Interactions with Materials and Atoms*, 286, pp. 346–350. doi: https://doi.org/10.1016/j.nimb.2012.01.032.

Garibaldi, C. *et al.* (2017) 'Recent advances in radiation oncology', Ecancermedicalscience (11) pp. 785.

Gensheimer, M. F. *et al.* (2010) 'In Vivo Proton Beam Range Verification Using Spine MRI Changes', *International Journal of Radiation Oncology Biology Physics*, 78(1), pp. 268–275. doi: 10.1016/j.ijrobp.2009.11.060.

Girdhani, S., Sachs, R. and Hlatky, L. (2013) 'Biological Effects of Proton Radiation: What We Know and Don't Know', *Radiation Research*, 179(3), pp. 257–272. doi: 10.1667/RR2839.1.

Goodhead, D. T. (1999) 'Mechanisms for the biological effectiveness of high-LET radiations.', *Journal of radiation research*, 40 Suppl, pp. 1–13.

Gottschalk, B. (2003) 'On the Characterization of Spread-Out Bragg Peaks and the Definition of " Depth " and " Modulation "', pp. 1–23.

Gravina, G. L. *et al.* (2010) 'Biological rationale for the use of DNA methyltransferase inhibitors as new strategy for modulation of tumor response to chemotherapy and radiation', *Molecular Cancer*. BioMed Central Ltd, 9(1), p. 305. doi: 10.1186/1476-4598-9-305.

Green, L. M. *et al.* (2001) 'Response of thyroid follicular cells to gamma irradiation compared to proton irradiation. I. Initial characterization of DNA damage, micronucleus formation, apoptosis, cell survival, and cell cycle phase redistribution.', *Radiation research*. United States, 155(1 Pt 1), pp. 32–42.

Gueulette, J. *et al.* (1997) 'RBE variation as a function of depth in the 200-MeV proton beam produced at the National Accelerator Centre in Faure (South Africa).', *Radiotherapy and oncology : journal of the European Society for Therapeutic Radiology and Oncology*, 42(3), pp. 303–309.

Guogytė, K. *et al.* (2017) 'Assessment of Correlation between Chromosomal Radiosensitivity of Peripheral Blood Lymphocytes after In vitro Irradiation and Normal Tissue Side Effects for Cancer Patients Undergoing Radiotherapy', *Genome Integrity*. India: Medknow Publications & Media Pvt Ltd, 8, p. 1. doi: 10.4103/2041-9414.198907.

Haas, J. A. *et al.* (2015) 'Stereotactic Body Radiation Therapy for Early-Stage Breast Cancer Using a Robotic Linear Accelerator', *Radiation Oncology Biology*. Elsevier Inc, 93(3), p. S61. doi: 10.1016/j.ijrobp.2015.07.145.

Haciislamoglu, E. *et al.* (2016) 'The choice of multi-beam IMRT for whole breast radiotherapy in early-stage right breast cancer', Pubmed 28;5(1):688. doi: 10.1186/s40064-016-2314-2.

Hall, E. J. (1985) 'Radiation biology.', *Cancer*, 55(9 Suppl), pp. 2051–2057. doi: 10.1007/s00247-008-1027-2.

Hall, E. J. and Cox, J. D. (2010) 'Chapter 1 - Physical and Biologic Basis of Radiation Therapy BT - Radiation Oncology (NINTH EDITION)', Philadelphia, pp. 3–49. doi: https://doi.org/.

Hawkins, R. B. (2009) 'The relationship between the sensitivity of cells to high-energy photons and the RBE of particle radiation used in radiotherapy.', *Radiation research*, 172(6), pp. 761–776. doi: 10.1667/RR1655.1.

Hawkins, R. B. (2017) 'Effect of heterogeneous radio sensitivity on the survival, alpha beta ratio and biologic effective dose calculation of irradiated mammalian cell populations', *Clinical and Translational Radiation Oncology*, 4, pp. 32–38. doi: https://doi.org/10.1016/j.ctro.2017.03.001.

Hayashi, M. (2016) 'The micronucleus test—most widely used in vivo genotoxicity test—', *Genes and Environment*. BioMed Central, 38, p. 18. doi: 10.1186/s41021-016-0044-x.

Hewitt, R. *et al.* (2007) 'Enhanced Micronucleus Formation and Modulation of Bcl-2:Bax in MCF-7 Cells after Exposure to Binary Mixtures', *Environmental Health Perspectives*. National Institute of Environmental Health Sciences, 115(Suppl 1), pp. 129–136. doi: 10.1289/ehp.9361.

Hill-Kayser, C. E., Both, S. and Tochner, Z. (2011) 'Proton Therapy: Ever Shifting Sands and the Opportunities and Obligations within', *Frontiers in Oncology*, 1(September), pp. 1–9. doi: 10.3389/fonc.2011.00024.

Hojo, H. *et al.* (2017) 'Difference in the relative biological effectiveness and DNA damage repair processes in response to proton beam therapy according to the positions of the spread out Bragg peak', *Radiation Oncology.* BioMed Central, 12, p. 111. doi: 10.1186/s13014-017-0849-1.

Hong, J. C. *et al.* (2017) 'Radiation dose and cardiac risk in breast cancer treatment: An analysis of modern radiation therapy including community settings.', *Practical radiation oncology*. doi: 10.1016/j.prro.2017.07.005.

Hooning, M. J. *et al.* (2006) 'Cause-specific mortality in long-term survivors of breast cancer: A 25-year follow-up study', *International Journal of Radiation Oncology Biology Physics*, 64(4), pp. 1081–1091. doi: 10.1016/j.ijrobp.2005.10.022.

Hooning, M. J. *et al.* (2007) 'Long-term risk of cardiovascular disease in 10-year survivors of breast cancer.', *Journal of the National Cancer Institute*, 99(5), pp. 365–375. doi: 10.1093/jnci/djk064.

Hosseini, M. A., Jia, S. B. and Ebrahimi-Loushab, M. (2017) 'Analysis of Relative Biological Effectiveness of Proton Beams and Iso-effective Dose Profiles Using Geant4 ', *Journal of Biomedical Physics & Engineering.* Journal of Biomedical Physics and Engineering, 7(2), pp. 95–100.

Hug, E. B. and Slater, J. D. (1999) 'Proton radiation therapy for pediatric malignancies: status report.', *Strahlentherapie und Onkologie : Organ der Deutschen Röntgengesellschaft ... [et al]*, 175 Suppl, pp. 89–91.

Ibanez, I. L. *et al.* (2009) 'Induction and rejoining of DNA double strand breaks assessed by H2AX phosphorylation in melanoma cells irradiated with proton and lithium beams.', *International journal of radiation oncology, biology, physics*, 74(4), pp. 1226–1235. doi: 10.1016/j.ijrobp.2009.02.070.

Ilicic, K., Combs, S. E. and Schmid, T. E. (2018) 'New insights in the relative radiobiological effectiveness of proton irradiation', *Radiation Oncology,* 13, p. 6. doi: 10.1186/s13014-018-0954-9.

Jacob, S. *et al.* (2016) 'Early detection and prediction of cardiotoxicity after radiation therapy for breast cancer: the BACCARAT prospective cohort study', *Radiation Oncology*, 11(1), p. 54. doi: 10.1186/s13014-016-0627-5.

Jacobson, G. M. *et al.* (2013) 'Mean radiation dose to the heart in patients with breast cancer.', *Journal of Clinical Oncology*. American Society of Clinical Oncology, 31(26_suppl), p. 56. doi: 10.1200/jco.2013.31.26_suppl.56.

Jaskowiak, N. (2014) 'Breast Cancer Control Policy, Department of Health South Africa', (June), pp. 1–57.

Jdey, W. *et al.* (2017) 'Micronuclei frequency in tumors is a predictive biomarker for genetic instability and sensitivity to the DNA repair inhibitor AsiDNA', *Cancer Research*, 77(16), pp. 4207–4216. doi: 10.1158/0008-5472.CAN-16-2693.

Jermann, M. (2017) 'Particle Therapy Patient Statistics (per end of 2016) (Data collected by the Particle Therapy Co-Operative Group)', *Ptcog*, 2017(December), pp. 2016–2017.

Joksic, G. *et al.* (2000) 'Chromosome aberrations, micronuclei, and activity of superoxide dismutases in human lymphocytes after irradiation in vitro.', *Cellular and molecular life sciences* . 57(5), pp. 842–850. doi: 10.1007/s000180050046.

Jones, B. (2015) 'Towards achieving the full clinical potential of proton therapy by inclusion of LET and RBE models', *Cancers*, 7(1), pp. 460–480. doi: 10.3390/cancers7010460.

Jones, B. (2016) 'Why RBE must be a variable and not a constant in proton therapy', *The British Journal of Radiology*. 89(1063), p. 20160116. doi: 10.1259/bjr.20160116.

Jones, B. (2017) 'Clinical radiobiology of proton therapy: modeling of RBE', *Acta Oncologica*. 56(11), pp. 1374–1378. doi: 10.1080/0284186X.2017.1343496.

Jones, B., McMahon, S. J. and Prise, K. M. (2018) 'The Radiobiology of Proton Therapy: Challenges and Opportunities Around Relative Biological Effectiveness.', *Clinical oncology.* 30(5), pp. 285–292. doi: 10.1016/j.clon.2018.01.010.

Kacprowska, A. and Jassem, J. (2012) 'Hypofractionated radiotherapy for early breast cancer: Review of phase III studies', *Reports of Practical Oncology & Radiotherapy*. 17(2), pp. 66–70. doi: 10.1016/J.RPOR.2011.10.003.

Kaidar-Person, O. *et al.* (2017) 'The incidence and predictive factors for leptomeningeal spread after stereotactic radiation for breast cancer brain metastases.', *The Breast Journal*. doi: 10.1111/tbj.12919.

Kaufman, E. L. *et al.* (2008) 'Effect of breast cancer radiotherapy and cigarette smoking on risk of second primary lung cancer.', *Journal of clinical oncology,* 26(3), pp. 392–398. doi: 10.1200/JCO.2007.13.3033.

Kooy, H. M. *et al.* (2003) 'Monitor unit calculations for range-modulated spread-out Bragg peak fields.', *Physics in medicine and biology,* 48(17), pp. 2797–2808.

Kozak, K. R. *et al.* (2006) 'Accelerated partial-breast irradiation using proton beams: initial clinical experience.', *International journal of radiation oncology, biology, physics*. 66(3), pp. 691–698. doi: 10.1016/j.ijrobp.2006.06.041.

Kuo, L. J. and Yang, L.-X. (2008) 'Gamma-H2AX - a novel biomarker for DNA double-strand breaks.', *In vivo* 22(3), pp. 305–309.

Laine, A. M. *et al.* (2015) 'The Role of Hypofractionated Radiation Therapy with Photons, Protons, and Heavy Ions for Treating Extracranial Lesions', *Frontiers in Oncology*. 5, p. 302. doi: 10.3389/fonc.2015.00302.

Lee, A. V, Oesterreich, S. and Davidson, N. E. (2015) 'MCF-7 cells--changing the course of breast cancer research and care for 45 years.', *Journal of the National Cancer Institute*. 107(7). doi: 10.1093/jnci/djv073.

van Leeuwen, C. M. *et al.* (2018) 'The alfa and beta of tumours: a review of parameters of the linear-quadratic model, derived from clinical radiotherapy studies', *Radiation Oncology.* 13, p. 96. doi: 10.1186/s13014-018-1040-z.

Levin, W. P. *et al.* (2005) 'Proton beam therapy', *British Journal of Cancer*, 93(8), pp. 849–854. doi: 10.1038/sj.bjc.6602754.

Lievens, Y. *et al.* (2015) 'Stereotactic Body Radiotherapy for Lung Cancer', *Journal of Thoracic Oncology*. 10(3), pp. 454–461. doi: 10.1097/JTO.0000000000000421.

Litière, S. *et al.* (2018) 'Breast conserving therapy versus mastectomy for stage I–II breast cancer: 20 year follow-up of the EORTC 10801 phase 3 randomised trial', *The Lancet Oncology*. 13(4), pp. 412–419. doi: 10.1016/S1470-2045(12)70042-6.

Lomax, A. J. *et al.* (2004) 'Treatment planning and verification of proton therapy using spot scanning: initial experiences.', *Medical physics*. 31(11), pp. 3150–3157. doi: 10.1118/1.1779371.

Lühr, A. *et al.* (2018) 'Relative biological effectiveness in proton beam therapy – current knowledge and future challenges', *Clinical and Translational Radiation Oncology*, (February), pp. 35–41. doi: 10.1016/j.ctro.2018.01.006.

MacDonald, S. M., Jimenez, R., *et al.* (2013) 'Proton radiotherapy for chest wall and regional lymphatic radiation; dose comparisons and treatment delivery', *Radiation Oncology*, 8(1), pp. 1–7. doi: 10.1186/1748-717X-8-71.

MacDonald, S. M., Patel, S. A., *et al.* (2013) 'Proton therapy for breast cancer after mastectomy: Early outcomes of a prospective clinical trial', *International Journal of Radiation Oncology Biology Physics*. 86(3), pp. 484–490. doi: 10.1016/j.ijrobp.2013.01.038.

Mailhot Vega, R. B. *et al.* (2016) 'Establishing Cost-Effective Allocation of Proton Therapy for Breast Irradiation.', *International journal of radiation oncology, biology, physics*. 95(1), pp. 11–18. doi: 10.1016/j.ijrobp.2016.02.031.

Malinen, E. and Sovik, A. (2015) 'Dose or "LET" painting--What is optimal in particle therapy of hypoxic tumors?', *Acta Oncologica.* 54(9), pp. 1614–1622. doi: 10.3109/0284186X.2015.1062540.

Marshall, T. I. *et al.* (2016) 'Investigating the Implications of a Variable RBE on Proton Dose Fractionation Across a Clinical Pencil Beam Scanned Spread-Out Bragg Peak', *International Journal of Radiation Oncology, Biology, Physics*. 95(1), pp. 70–77. doi: 10.1016/j.ijrobp.2016.02.029.

Martinez-Planell, R., Lopez Torres, J. and Robles Hernandez, I. (2015) *Students' understanding of quadratic equations*, *International Journal of Mathematics Education in Science and Techonology*. doi: 10.1080/0020739X.2015.1119895.

Mason, A. J. *et al.* (2011) 'Interaction between the biological effects of high- and low-LET radiation dose components in a mixed field exposure.', *International journal of radiation biology*. 87(12), pp. 1162–1172. doi: 10.3109/09553002.2011.624154.

Mast, M. E. *et al.* (2014) 'Whole breast proton irradiation for maximal reduction of heart dose in breast cancer patients.', *Breast cancer research and treatment*. 148(1), pp. 33–39. doi: 10.1007/s10549-014-3149-6.

McMahon, S. J. *et al.* (2016) 'Mechanistic Modelling of DNA Repair and Cellular Survival Following Radiation-Induced DNA Damage', *Scientific Reports*. 6, p. 33290.

Mcnamara, A. L. *et al.* (2012) 'Range uncertainty in proton therapy due to variable'. doi: 10.1088/0031-9155/57/5/1159.

McNamara, A. (2015) 'A phenomenological relative biological effectiveness (RBE) model for proton therapy based on all published in vitro cell survival data', *Physics in medicine and biology*, 60(21), pp. 8399–8416. doi: 10.1088/0031-9155/60/21/8399.

Miller, K. D. *et al.* (2016) 'Cancer Treatment and Survivorship Statistics , 2016', 66(4), pp. 271–289. A Cancer Journal for Clinicians. doi: 10.3322/caac.21349.

Mognato, M. *et al.* (2003) 'Genetic damage induced by in vitro irradiation of human G0 lymphocytes with low-energy protons (28 keV/microm): HPRT mutations and chromosome aberrations.', *Radiation research*. 160(1), pp. 52–60.

Mohan, R. *et al.* (2017) 'Radiobiological issues in proton therapy', *Acta oncologica (Stockholm, Sweden)*, 56(11), pp. 1367–1373. doi: 10.1080/0284186X.2017.1348621.

Moignier, A. *et al.* (2014) 'Dependence of coronary 3-dimensional dose maps on coronary topologies and beam set in breast radiation therapy: a study based on CT angiographies', *International Journal Radiation Oncolology and Biological Physics*, 89. doi: 10.1016/j.ijrobp.2014.01.055.

Murugan, N. *et al.* (2014) 'Down-staging of breast cancer in the pre-screening era : Experiences from Chris Hani Baragwanath Academic Hospital , Soweto , South Africa',South African Medical Journal.

104(5), pp. 2012–2015. doi: 10.7196/SAMJ.8243.

Narod, S. A., Iqbal, J. and Miller, A. B. (2015) 'Why have breast cancer mortality rates declined ?', *Journal of Cancer Policy*. 5, pp. 8–17. doi: 10.1016/j.jcpo.2015.03.002.

Newhauser, W. (2009) *ICRUPrescribing, Recording and Reporting Photon Beam Therapy. International Commissions on Radiation Units and Measurements (Supplement to ICRU Report 50): Bethesda, MD, USA. Report 62*, *Radiation Protection Dosimetry.* doi: 10.1093/rpd/ncp005.

Nichiporov, D., Hsi, W. and Farr, J. (2012) 'Beam characteristics in two different proton uniform scanning systems: A side-by-side comparison', *Medical Physics*. 39(5), pp. 2559–2568. doi: 10.1118/1.3701774.

Nilsson, G. *et al.* (2012) 'Distribution of coronary artery stenosis after radiation for breast cancer', *J Clin Oncol*, 30(4):380-6. doi: 10.1200/JCO.2011.34.5900.

Nissen, H. D. and Appelt, A. L. (2013) 'Improved heart, lung and target dose with deep inspiration breath hold in a large clinical series of breast cancer patients.', *Radiotherapy and oncology : journal of the European Society for Therapeutic Radiology and Oncology*. 106(1), pp. 28–32. doi: 10.1016/j.radonc.2012.10.016.

Norppa, H. and Falck, G. C.-M. (2003) 'What do human micronuclei contain?', *Mutagenesis*. 18(3), pp. 221–233.

Ottoboni, C. *et al.* (2001) 'Induction of micronuclei by a new non-peptidic mimetic farnesyltransferase inhibitor RPR-115135: role of gene mutations', *Mutagenesis*, 16(5), pp. 423–430.

Paganetti, H. *et al.* (2002) 'Relative biological effectiveness (RBE) values for proton beam therapy', *International Journal of Radiation Oncology Biology Physics*. 53(2), pp. 407–421. doi: 10.1016/S0360-3016(02)02754-2.

Paganetti, H. (2003) 'Significance and implementation of RBE variations in proton beam therapy.', *Technology in cancer research & treatment*. 2(5), pp. 413–426. doi: 10.1177/153303460300200506.

Paganetti, H. (2014) 'Relative biological effectiveness (RBE) values for proton beam therapy. Variations as a function of biological endpoint, dose, and linear energy transfer', *Physics in Medicine and Biology*, 59(22), pp. R419–R472. doi: 10.1088/0031-9155/59/22/R419.

Pajonk, F. (2010) 'Radiation Resistance of Cancer Stem Cells: The 4 R's of Radiobiology Revisited', *Stem cells.* 28(4), pp. 639–648. doi: 10.1002/stem.318.

Pan, H. *et al.* (2011) 'A Survey of Stereotactic Body Radiation Therapy Use in the United States', *Cancer*, pp. 4566–4572. doi: 10.1002/cncr.26067.

Parag, Y. and Buccimazza, I. (2016) 'How long are elderly patients followed up with mammography after the diagnosis of breast cancer? A single-centre experience in a developing country', *South African Medical Journal*, 106(7), p. 721. doi: 10.7196/SAMJ.2016.v106i7.10405.

Prochazka, M. *et al.* (2002) 'Lung cancer risks in women with previous breast cancer.', *European journal of cancer.* 38(11), pp. 1520–1525.

PTCOG (2018) *Particle Therapy Centers*, *online*. Available at: https://www.ptcog.ch/index.php/facilities-in-planning-stage (Accessed: 26 September 2018).

Rabinovitch, P. S. (1994) 'DNA content histogram and cell-cycle analysis.', *Methods in cell biology*. 41, pp. 263–296.

Ray, K. J., Sibson, N. R. and Kiltie, A. E. (2015) 'Treatment of Breast and Prostate Cancer by Hypofractionated Radiotherapy: Potential Risks and Benefits', *Clinical Oncology.* 27(7), pp. 420–426. doi: 10.1016/j.clon.2015.02.008.

Redon, C. E. *et al.* (2009) 'gamma-H2AX as a biomarker of DNA damage induced by ionizing radiation in human peripheral blood lymphocytes and artificial skin.', *Advances in space research : the official journal of the Committee on Space Research (COSPAR)*. 43(8), pp. 1171–1178. doi:

10.1016/j.asr.2008.10.011.

Rothfuss, A. *et al.* (2000) 'Induced Micronucleus Frequencies in Peripheral Lymphocytes as a Screening Test for Carriers of a BRCA1 Mutation in Breast Cancer Families Induced Micronucleus Frequencies in Peripheral Lymphocytes as a Screening Test for Carriers of a BRCA1 Mutation in Br', Cancer Research. pp. 390–394.

Sakthivel, V. *et al.* (2017) 'Radiation-Induced Second Cancer Risk from External Beam Photon Radiotherapy for Head and Neck Cancer: Impact on in-Field and Out-of-Field Organs', *Asian Pacific Journal of Cancer Prevention.* 18(7), pp. 1897–1903. doi: 10.22034/APJCP.2017.18.7.1897.

Schmid, E., Schraube, H. and Bauchinger, M. (1998) 'Chromosome aberration frequencies in human lymphocytes irradiated in a phantom by a mixed beam of fission neutrons and gamma-rays.', *International journal of radiation biology*. 73(3), pp. 263–267.

Scholz, M. and Elsässer, T. (2007) 'Biophysical models in ion beam radiotherapy', *Advances in Space Research*, 40(9), pp. 1381–1391. doi: https://doi.org/10.1016/j.asr.2007.02.066.

Scott, D. *et al.* (1999) 'Increased chromosomal radiosensitivity in breast cancer patients: A comparison of two assays', *International Journal of Radiation Biology*, 75(1), pp. 1–10. doi: 10.1080/095530099140744.

Sgura, A. *et al.* (2000) 'Micronuclei, CREST-positive micronuclei and cell inactivation induced in Chinese hamster cells by radiation with different quality.', *International journal of radiation biology*, 76(3), pp. 367–74. doi: 10.1080/095530000138709.

Shao, C. *et al.* (2008) 'Estrogen enhanced cell-cell signalling in breast cancer cells exposed to targeted irradiation', *BMC Cancer*. 8, p. 184. doi: 10.1186/1471-2407-8-184.

Slabbert, J. *et al.* (2015) 'Increased Proton Relative Biological Effectiveness at the Very End of a Spread-Out Bragg Peak for Jejunum Irradiated Ex Vivo', *International Journal of Particle Therapy*, 2(1), pp. 37–43. doi: 10.14338/IJPT-14-00027.1.

Smit, K. A., *In Vitro Prediction of Inherent Cellular Radiosensitivity*, 2005, Department of Biomedical Technology, Faculty of Applied Sciences, Cape Technikon, Thesis: Master Technologiae (Biomedical Technology), http://etd.cput.ac.za/bitstream/handle/20.500.11838/1492/In%20vitro%20prediction%20of%20inherit%20cellular%20radiosensitivity.pdf?sequence=1&isAllowed=y.

Sørensen, B. S. *et al.* (2017) 'Relative biological effectiveness (RBE) and distal edge effects of proton radiation on early damage in vivo', *Acta Oncologica*. 56(11), pp. 1387–1391. doi: 10.1080/0284186X.2017.1351621.

Sorensen, B. S., Overgaard, J. and Bassler, N. (2011) 'In vitro RBE-LET dependence for multiple particle types.', *Acta oncologica* 50(6), pp. 757–762. doi: 10.3109/0284186X.2011.582518.

Strom, E. A. and Ovalle, V. (2014) 'Initial Clinical Experience Using Protons for Accelerated Partial-Breast Irradiation: Longer-term Results', *International Journal of Radiation Oncology Biology Physics*. 90(3), pp. 506–508. doi: 10.1016/j.ijrobp.2014.06.039.

Taylor, C. W. *et al.* (2007) 'Cardiac exposures in breast cancer radiotherapy: 1950s-1990s', *International Journal of Radiation Oncology and Biology Physics*, 69. doi: 10.1016/j.ijrobp.2007.05.034.

Terzoudi, G. I. and Pantelias, G. E. (2006) 'Cytogenetic methods for biodosimetry and risk individualisation after exposure to ionising radiation', *Radiation Protection Dosimetry*, 122(1–4), pp. 513–520. doi: 10.1093/rpd/ncl509.

Theron, T. *et al.* (1997) 'The merits of cell kinetic parameters for the assessment of intrinsic cellular radiosensitivity to photon and high linear energy transfer neutron irradiation', *International Journal of Radiation Oncology Biology Physics*. 37(2), pp. 423–428. doi: 10.1016/S0360-3016(96)00533-0.

Titt, U. *et al.* (2017) 'Technical Note: Dosimetric characteristics of the ocular beam line and

commissioning data for an ocular proton therapy planning system at the Proton Therapy Center Houston.', *Medical physics*. 44(12), pp. 6661–6671. doi: 10.1002/mp.12605.

Todorov, S. L. *et al.* (1972) 'Dose-response relationship for chromosome aberrations induced by x-rays or 50 MeV protons in human peripheral lymphocytes.', *Mutation research*. 15(2), pp. 215–220.

Tommasino, F. and Durante, M. (2015) 'Proton radiobiology', *Cancers*, 7(1), pp. 353–381. doi: 10.3390/cancers7010353.

Tyran, M. *et al.* (2015) 'Volumetric-modulated arc therapy for left-sided breast cancer and all regional nodes improves target volumes coverage and reduces treatment time and doses to the heart and left coronary artery , compared with a field-in- field technique', Journal of Readiation Research, 56(6), pp. 927–937. doi: 10.1093/jrr/rrv052.

Underwood, T. and Paganetti, H. (2018) 'Variable Proton Relative Biological Effectiveness: How Do We Move Forward?', *International Journal of Radiation Oncology Biology Physics*. 95(1), pp. 56–58. doi: 10.1016/j.ijrobp.2015.10.006.

Urano, M. *et al.* (1984) 'Relative biological effectiveness of modulated proton beams in various murine tissues', *International Journal of Radiation Oncology Biology Physics*. 10(4), pp. 509–514. doi: 10.1016/0360-3016(84)90031-2.

Vandersickel, V. *et al.* (2010) 'The radiosensitizing effect of Ku70/80 knockdown in MCF10A cells irradiated with X-rays and p(66)+Be(40) neutrons', *Radiation Oncology.* p. 30. doi: 10.1186/1748-717X-5-30.

Veronesi, U. *et al.* (2002) 'Twenty-Year Follow-up of a Randomized Study Comparing Breast-Conserving Surgery with Radical Mastectomy for Early Breast Cancer', *New England Journal of Medicine*. 347(16), pp. 1227–1232. doi: 10.1056/NEJMoa020989.

Villagrasa, C. *et al.* (2014) 'RBE-LET relationship for proton and alpha irradiations studied with a nanodosimetric approach.', *Radiation protection dosimetry*. 161(1–4), pp. 449–453. doi: 10.1093/rpd/ncu047.

Vral, A., Fenech, M. and Thierens, H. (2011) 'The micronucleus assay as a biological dosimeter of in vivo ionising radiation exposure', *Mutagenesis*, 26(1), pp. 11–17.

Wang, D. (2015) 'A critical appraisal of the clinical utility of proton therapy in oncology', *Medical Devices.* 8, pp. 439–446. doi: 10.2147/MDER.S65594.

Wedenberg, M. and Toma-Dasu, I. (2014) 'Disregarding RBE variation in treatment plan comparison may lead to bias in favor of proton plans.', *Medical physics*. 41(9), p. 91706. doi: 10.1118/1.4892930.

Weyrather, W. K. *et al.* (1999) 'RBE for carbon track-segment irradiation in cell lines of differing repair capacity.', *International journal of radiation biology*. 75(11), pp. 1357–1364.

Whalen, M. K. *et al.* (2008) 'Specific ATM-Mediated Phosphorylation Dependent on Radiation Quality', *Radiation Research*. 170(3), pp. 353–364. doi: 10.1667/RR1354.1.

Wilkens, J. J. and Oelfke, U. (2004) 'Three-dimensional LET calculations for treatment planning of proton therapy.', *Zeitschrift fur medizinische Physik*. 14(1), pp. 41–46.

Wroe, A. J., Bush, D. A. and Slater, J. D. (2014) 'Immobilization Considerations for Proton Radiation Therapy', *Technology in Cancer Research & Treatment*, 13(3), pp. 217–226. doi: 10.7785/tcrt.2012.500376.

Wu, H. *et al.* (1997) 'Induction of Chromosome Aberrations in Human Cells by Charged Particles', *Radiation Research*. 148(5), pp. S102–S107. doi: 10.2307/3579723.

Xu, N. *et al.* (2014) 'Can proton therapy improve the therapeutic ratio in breast cancer patients at risk for nodal disease?', *American journal of clinical oncology*. 37(6), pp. 568–574. doi: 10.1097/COC.0b013e318280d614.

Yang, H., Anzenberg, V. and Held, K. D. (2007) 'Effects of heavy ions and energetic protons on normal

human fibroblasts.', *Radiatsionnaia biologiia, radioecologiia*. 47(3), pp. 302–306.

Yang, M. *et al.* (2012) 'Comprehensive analysis of proton range uncertainties related to patient stopping-power-ratio estimation using the stoichiometric calibration', *Physics in Medicine and Biology*, 57(13), pp. 4095–4115. doi: 10.1088/0031-9155/57/13/4095.

Yarnold, J. (2018) 'Changes in radiotherapy fractionation-breast cancer.', *The British journal of radiology*. p. 20170849. doi: 10.1259/bjr.20170849.

Yashar, C. M. (2012) 'Chapter 23 - Basic Principles in Gynecologic Radiotherapy A2 - Saia, Philip J. Di', in Creasman, (Eighth E. (ed.). Philadelphia: Mosby, p. 659–680.e3. doi: https://doi.org/10.1016/B978-0-323-07419-3.00023-0.

Yu, C. X. *et al.* (2013) 'GammaPod—A new device dedicated for stereotactic radiotherapy of breast cancer', *Medical Physics*. doi: 10.1118/1.4798961.

Yusuf, S. W. *et al.* (2017) 'Radiation-Induced Cardiovascular Disease: A Clinical Perspective', *Frontiers in Cardiovascular Medicine*. 4, p. 66. doi: 10.3389/fcvm.2017.00066.

Zagar, T. M., Cardinale, D. M. and Marks, L. B. (2016) 'Breast cancer therapy-associated cardiovascular disease.', *Nature reviews. Clinical oncology*. 13(3), pp. 172–184. doi: 10.1038/nrclinonc.2015.171.

Zhang, R. and Newhauser, W. D. (2009) 'Calculation of water equivalent thickness of materials of arbitrary density, elemental composition and thickness in proton beam irradiation', *Physics in medicine and biology*, 54(6), pp. 1383–1395. doi: 10.1088/0031-9155/54/6/001.

Zhang, X. *et al.* (2013) 'Therapy resistant cancer stem cells have differing sensitivity to photon versus proton beam radiation', *Journal of thoracic oncology : official publication of the International Association for the Study of Lung Cancer*, 8(12), p. 10.1097/JTO.0b013e3182a5fdcb. doi: 10.1097/JTO.0b013e3182a5fdcb.

Zhao, L. *et al.* (2017) 'Radiosensitivity and relative biological effectiveness based on a generalized target model', *Journal of Radiation Research*, 58(1), pp. 8–16. doi: 10.1093/jrr/rrw062.